INFRASTRUTTURE VIARIE IN SOTTERRANEO

IN SITU AND INDUCED STRESSES

Prof. Ing. Geol. Eugenio Castelli

ecastelli@units.it

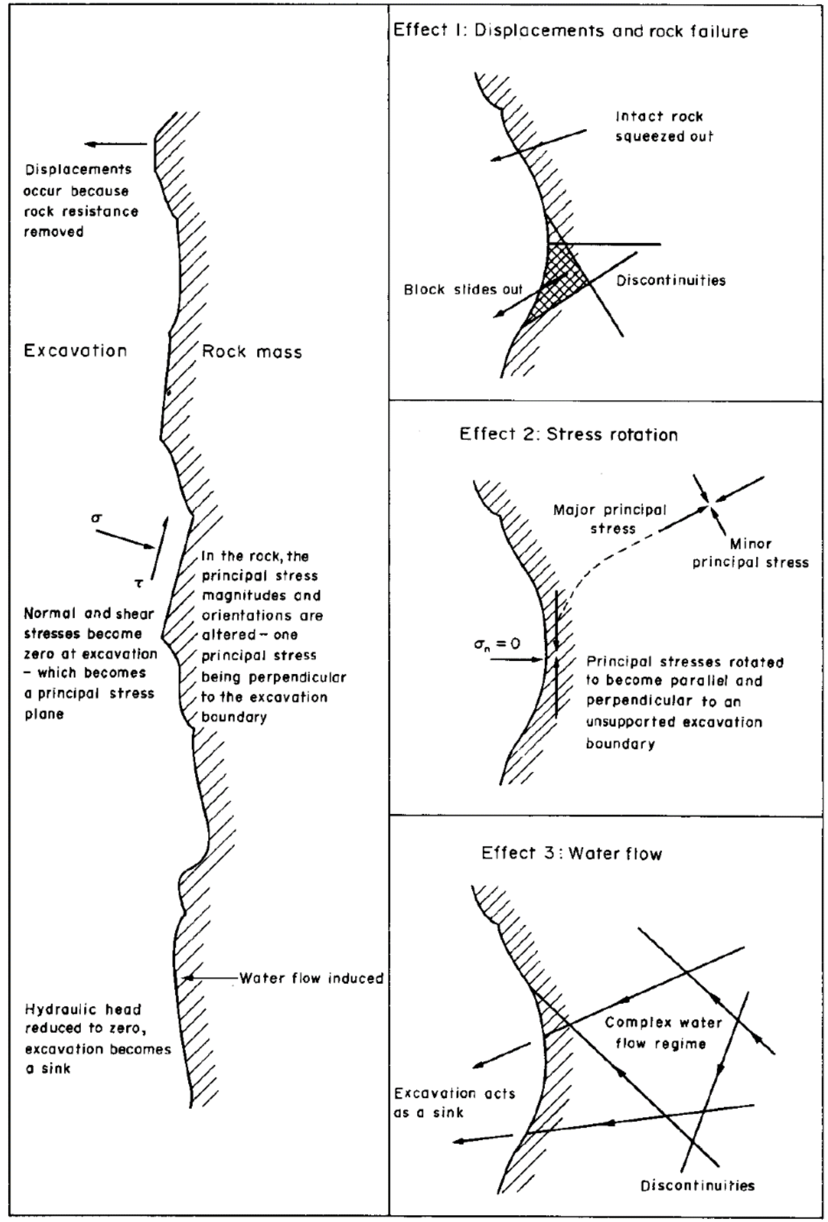

Figure 30 The three primary effects of excavation

Not only are the principal stresses and their directions of fundamental significance in stress analysis, the concept of a principal stress also has particular significance for rock engineering. This is because *all unsupported excavation surfaces,* whether at the ground surface or underground, have no

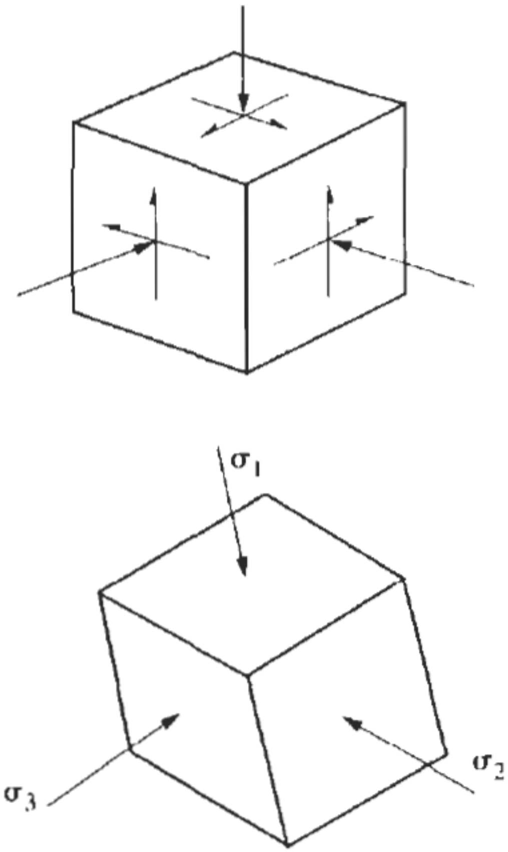

$$\begin{bmatrix} \sigma_{xx} & \tau_{xy} & \tau_{xz} \\ \tau_{yx} & \sigma_{yy} & \tau_{yz} \\ \tau_{zx} & \tau_{zy} & \sigma_{zz} \end{bmatrix}$$

$$\begin{bmatrix} \sigma_1 & 0 & 0 \\ 0 & \sigma_2 & 0 \\ 0 & 0 & \sigma_3 \end{bmatrix}$$

Figure 3.7 The stress components on the reference cube and the principal stress components.

shear stresses acting on them and are therefore principal stress planes. This results from Newton's Third Law ('to every action there is an equal and opposite reaction'). Furthermore, and also from Newton's Third Law, the normal stress component acting on such surfaces is zero. Thus, we know at the outset that the stress state at all unsupported excavation surfaces will be

$$\begin{bmatrix} \sigma_{xx} & \tau_{xy} & \tau_{xz} \\ \tau_{yx} & \sigma_{yy} & \tau_{yz} \\ \tau_{zx} & \tau_{zy} & \sigma_{zz} \end{bmatrix}.$$

or in principal stress notation

$$\begin{bmatrix} 0 & 0 & 0 \\ 0 & \sigma_1 & 0 \\ 0 & 0 & \sigma_2 \end{bmatrix}$$

expressed, respectively, relative to an x-, y-, z-axes system with x perpendicular to the face, and the principal stresses acting as shown in Fig. 3.8.

In Fig. 3.8(a), the pre-existing stress state is shown in terms of the principal stresses. In Fig. 3.8(b) the stress state has been affected by excavation: both the magnitudes and directions of the principal stresses have changed. Neglecting atmospheric pressure, all stress components acting on the air–rock interface must be zero.

It should also be noted that the air–rock interface could be the surface of an open fracture in the rock mass itself. Thus, as we will discuss further in Chapters 4, 7 and 14, the rock mass structure can have a significant effect on the local stress distribution.

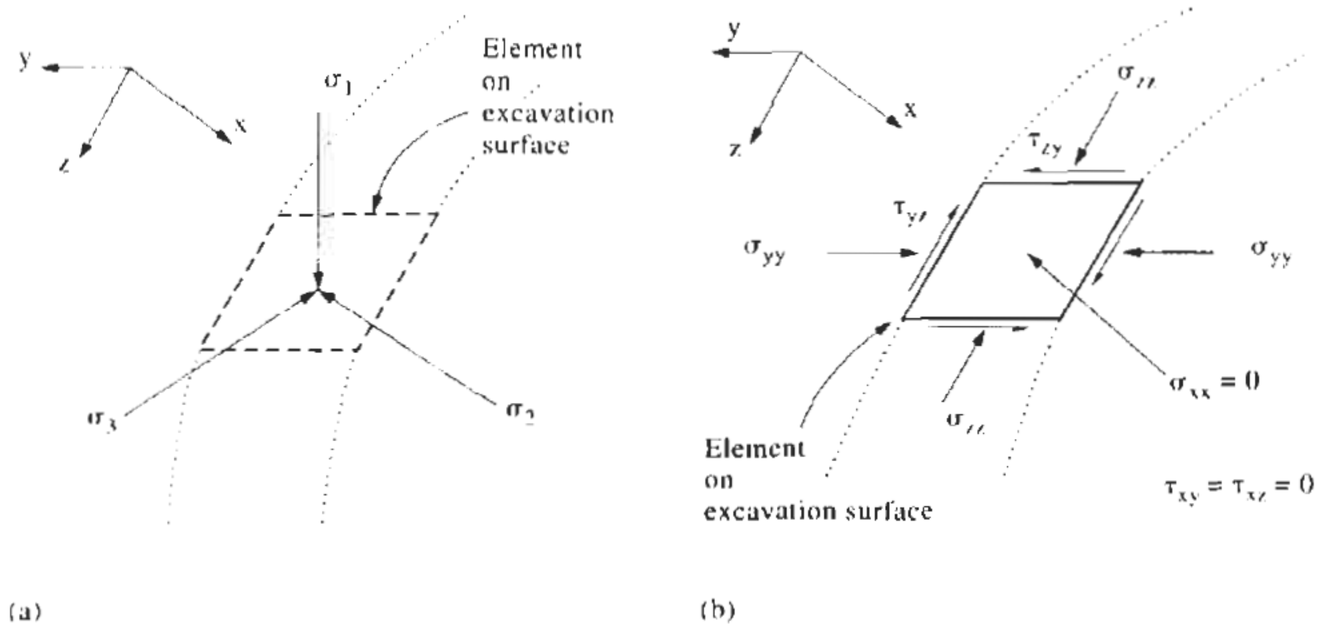

Figure 3.8 (a) Before excavation. (b) After excavation.

Introduction

Rock at depth is subjected to stresses resulting from the weight of the overlying strata and from locked in stresses of tectonic origin. When an opening is excavated in this rock, the stress field is locally disrupted and a new set of stresses are induced in the rock surrounding the opening. Knowledge of the magnitudes and directions of these in situ and induced stresses is an essential component of underground excavation design since, in many cases, the strength of the rock is exceeded and the resulting instability can have serious consequences on the behaviour of the excavations.

This chapter deals with the question of in situ stresses and also with the stress changes that are induced when tunnels or caverns are excavated in stressed rock. Problems, associated with failure of the rock around underground openings and with the design of support for these openings, will be dealt with in later chapters.

The presentation, which follows, is intended to cover only those topics which are essential for the reader to know about when dealing with the analysis of stress induced instability and the design of support to stabilise the rock under these conditions.

In situ stresses

Consider an element of rock at a depth of 1,000 m below the surface. The weight of the vertical column of rock resting on this element is the product of the depth and the unit weight of the overlying rock mass (typically about 2.7 tonnes/m^3 or 0.027 MN/m^3). Hence the vertical stress on the element is 2,700 tonnes/m^2 or 27 MPa. This stress is estimated from the simple relationship:

$$\sigma_v = \gamma z \qquad (1)$$

where σ_v is the vertical stress
γ is the unit weight of the overlying rock and
z is the depth below surface.

Measurements of vertical stress at various mining and civil engineering sites around the world confirm that this relationship is valid although, as illustrated in Figure 1, there is a significant amount of scatter in the measurements.

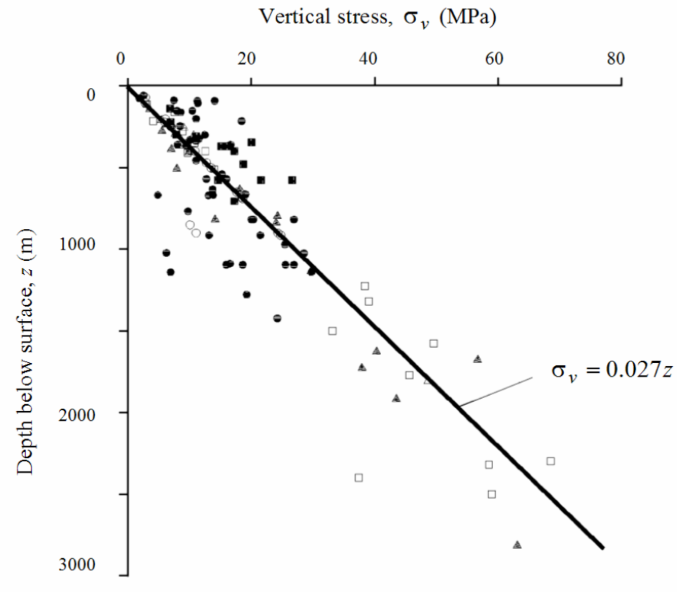

Figure 1: Vertical stress measurements from mining and civil engineering projects around the world. (After Brown and Hoek 1978).

The horizontal stresses acting on an element of rock at a depth z below the surface are much more difficult to estimate than the vertical stresses. Normally, the ratio of the average horizontal stress to the vertical stress is denoted by the letter k such that:

$$\sigma_h = k\sigma_v = k\gamma z \qquad (2)$$

Terzaghi and Richart (1952) suggested that, for a gravitationally loaded rock mass in which no lateral strain was permitted during formation of the overlying strata, the value of k is independent of depth and is given by $k = \nu/(1-\nu)$, where ν is the Poisson's ratio of the rock mass. This relationship was widely used in the early days of rock mechanics but, as discussed below, it proved to be inaccurate and is seldom used today.

Measurements of horizontal stresses at civil and mining sites around the world show that the ratio k tends to be high at shallow depth and that it decreases at depth (Brown and Hoek, 1978, Herget, 1988). In order to understand the reason for these horizontal stress variations it is necessary to consider the problem on a much larger scale than that of a single site.

Sheorey (1994) developed an elasto-static thermal stress model of the earth. This model considers curvature of the crust and variation of elastic constants, density and thermal expansion coefficients through the crust and mantle. A detailed discussion on Sheorey's model is beyond the scope of this chapter, but he did provide a simplified equation which can be used for estimating the horizontal to vertical stress ratio k. This equation is:

$$k = 0.25 + 7E_h\left(0.001 + \frac{1}{z}\right) \tag{3}$$

where z (m) is the depth below surface and E_h (GPa) is the average deformation modulus of the upper part of the earth's crust measured in a horizontal direction. This direction of measurement is important particularly in layered sedimentary rocks, in which the deformation modulus may be significantly different in different directions.

A plot of this equation is given in Figure 2 for a range of deformation moduli. The curves relating k with depth below surface z are similar to those published by Brown and Hoek (1978), Herget (1988) and others for measured in situ stresses. Hence equation 3 is considered to provide a reasonable basis for estimating the value of k.

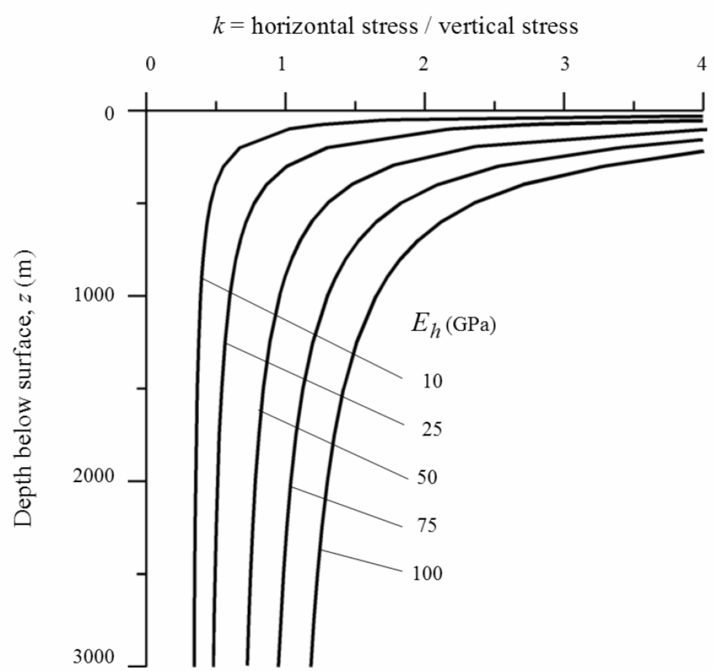

Figure 2: Ratio of horizontal to vertical stress for different deformation moduli based upon Sheorey's equation. (After Sheorey 1994).

As pointed out by Sheorey, his work does not explain the occurrence of measured vertical stresses that are higher than the calculated overburden pressure, the presence of very high horizontal stresses at some locations or why the two horizontal stresses are seldom equal. These differences are probably due to local topographic and geological features that cannot be taken into account in a large scale model such as that proposed by Sheorey.

Where sensitivity studies have shown that the in situ stresses are likely to have a significant influence on the behaviour of underground openings, it is recommended that the in situ stresses should be measured. Suggestions for setting up a stress measuring programme are discussed later in this chapter.

The World stress map

The World Stress Map project, completed in July 1992, involved over 30 scientists from 18 countries and was carried out under the auspices of the International Lithosphere Project (Zoback, 1992). The aim of the project was to compile a global database of contemporary tectonic stress data.

The World Stress Map (WSM) is now maintained and it has been extended by the Geophysical Institute of Karlsruhe University as a research project of the Heidelberg Academy of Sciences and Humanities. The 2005 version of the map contains approximately 16,000 data sets and various versions of the map for the World, Europe, America, Africa, Asia and Australia can be downloaded from the Internet. The WSM is an open-access database that can be accessed at www.world-stress-map.org (Reinecker et al, 2005)

The 2005 World Stress Map is reproduced in Figure 3 while a stress map for the Mediterranean is reproduced in Figure 4.

The stress maps display the orientations of the maximum horizontal compressive stress. The length of the stress symbols represents the data quality, with A being the best quality. Quality A data are assumed to record the orientation of the maximum horizontal compressive stress to within 10°-15°, quality B data to within 15°-20°, and quality C data to within 25°. Quality D data are considered to give questionable tectonic stress orientations.

The 1992 version of the World Stress Map was derived mainly from geological observations on earthquake focal mechanisms, volcanic alignments and fault slip interpretations. Less than 5% of the data was based upon hydraulic fracturing or overcoring measurements of the type commonly used in mining and civil engineering projects. In contrast, the 2005 version of the map includes a significantly greater number of observations from borehole break-outs, hydraulic fracturing, overcoring and borehole slotting. It is therefore worth considering the relative accuracy of these measurements as compared with the geological observations upon which the original map was based.

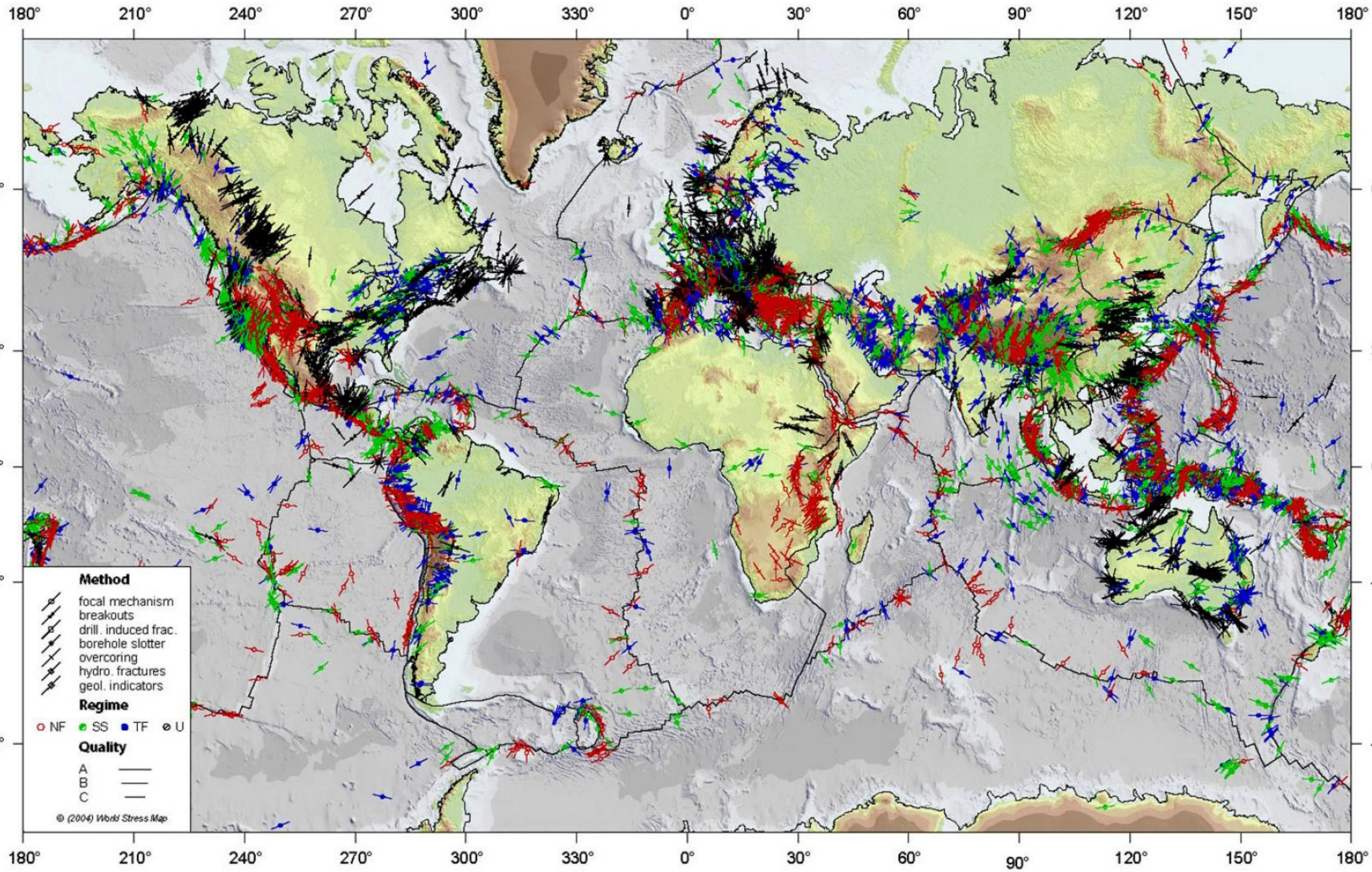

Figure 3: World stress map giving orientations of the maximum horizontal compressive stress. From www.world-stress-map.org.

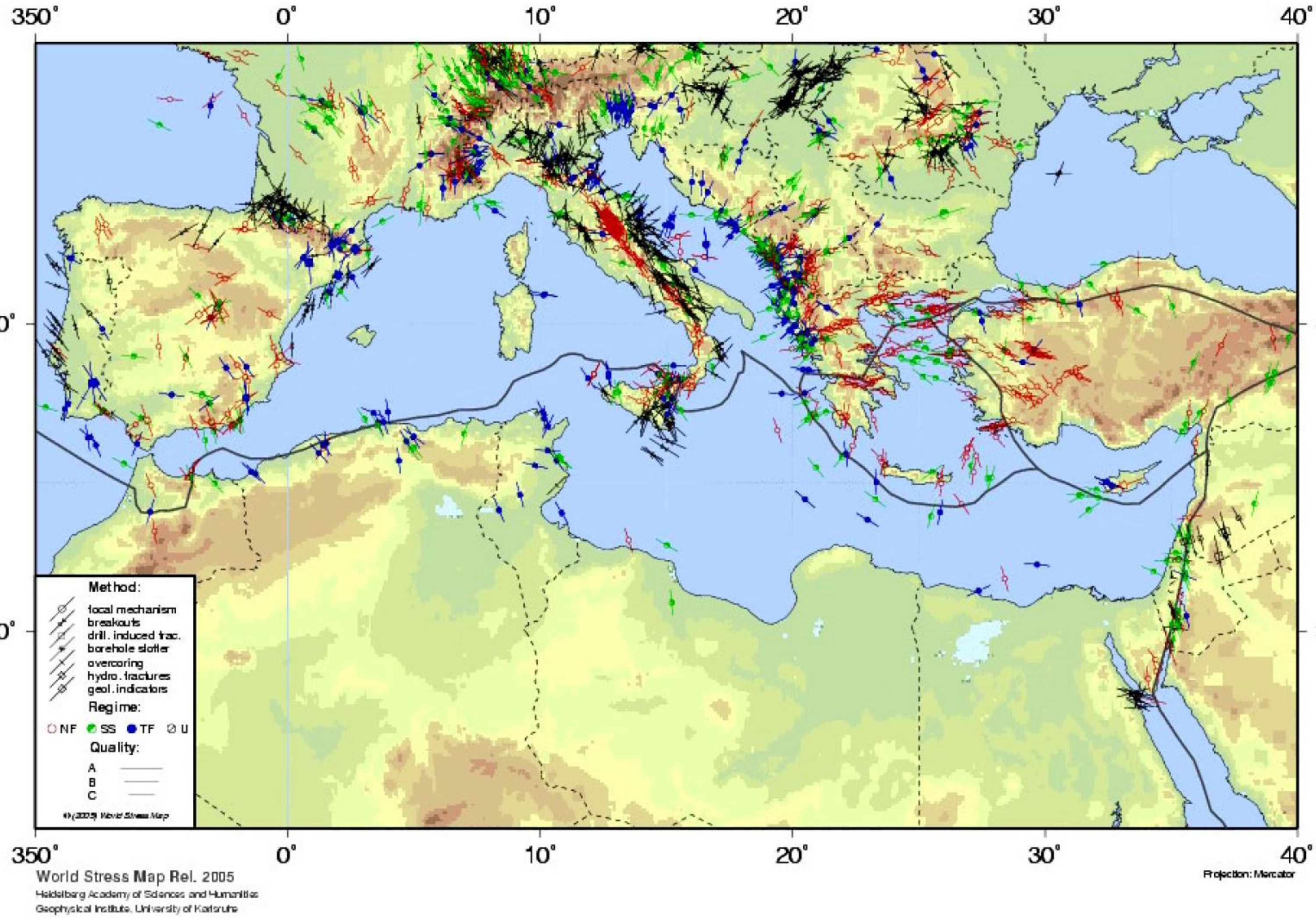

Figure 4: Stress map of the Mediterranean giving orientations of the maximum horizontal compressive stress. From www.world-stress-map.org.

In discussing hydraulic fracturing and overcoring stress measurements, Zoback (1992) has the following comments:

> 'Detailed hydraulic fracturing testing in a number of boreholes beginning very close to surface (10-20 m depth) has revealed marked changes in stress orientations and relative magnitudes with depth in the upper few hundred metres, possibly related to effects of nearby topography or a high degree of near surface fracturing.
>
> Included in the category of 'overcoring' stress measurements are a variety of stress or strain relief measurement techniques. These techniques involve a three-dimensional measurement of the strain relief in a body of rock when isolated from the surrounding rock volume; the three-dimensional stress tensor can subsequently be calculated with a knowledge of the complete compliance tensor of the rock. There are two primary drawbacks with this technique which restricts its usefulness as a tectonic stress indicator: measurements must be made near a free surface, and strain relief is determined over very small areas (a few square millimetres to square centimetres). Furthermore, near surface measurements (by far the most common) have been shown to be subject to effects of local topography, rock anisotropy, and natural fracturing (Engelder and Sbar, 1984). In addition, many of these measurements have been made for specific engineering applications (e.g. dam site evaluation, mining work), places where topography, fracturing or nearby excavations could strongly perturb the regional stress field.'

Obviously, from a global or even a regional scale, the type of engineering stress measurements carried out in a mine or on a civil engineering site are not regarded as very reliable. Conversely, the World Stress Map versions presented in Figures 3 and 4 can only be used to give first order estimates of the stress directions which are likely to be encountered on a specific site. Since both stress directions and stress magnitudes are critically important in the design of underground excavations, it follows that a stress measuring programme may be required in any major underground mining or civil engineering project.

Developing a stress measuring programme

Consider the example of a tunnel to be driven a depth of 1,000 m below surface in a hard rock environment. The depth of the tunnel is such that it is probable that in situ and induced stresses will be an important consideration in the design of the excavation. Typical steps that could be followed in the analysis of this problem are:

The World Stress Map for the area under consideration will give a good first indication of the possible complexity of the regional stress field and possible directions for the maximum horizontal compressive stress.

1. During preliminary design, the information presented in equations 1 and 3 can be used to obtain a first rough estimate of the vertical and average horizontal stress in the vicinity of the tunnel. For a depth of 1,000 m, these equations give the vertical stress σ_v = 27 MPa, the ratio k = 1.3 (for E_h = 75 GPa) and hence the average horizontal stress σ_h= 35.1 MPa. A preliminary analysis of the stresses induced around the proposed tunnel shows that these induced stresses are likely to exceed the strength of the rock and that the question of stress measurement must be considered in more detail. Note that for many openings in strong rock at shallow depth, stress problems may not be significant and the analysis need not proceed any further.

For this particular case, stress problems are considered to be important. A typical next step would be to search the literature in an effort to determine whether the results of in situ stress measurement programmes are available for mines or civil engineering projects within a radius of say 50 km of the site. With luck, a few stress measurement results will be available for the region in which the tunnel is located and these results can be used to refine the analysis discussed above.

Assuming that the results of the analysis of induced stresses in the rock surrounding the proposed tunnel indicate that significant zones of rock failure are likely to develop, and that support costs are likely to be high, it is probably justifiable to set up a stress measurement project on the site. These measurements can be carried out in deep boreholes from the surface, using hydraulic fracturing techniques, or from underground access using overcoring methods. The choice of the method and the number of measurements to be carried out depends upon the urgency of the problem, the availability of underground access and the costs involved in the project. Note that very few project organisations have access to the equipment required to carry out a stress measurement project and, rather than purchase this equipment, it may be worth bringing in an organisation which has the equipment and which specialises in such measurements.

2. Where regional tectonic features such as major faults are likely to be encountered the in situ stresses in the vicinity of the feature may be rotated with respect to the regional stress field. The stresses may be significantly different in magnitude from the values estimated from the general trends described above. These differences can be very important in the design of the openings and in the selection of support and, where it is suspected that this is likely to be the case, in situ stress measurements become an essential component of the overall design process.

Lower Kihansi Hydropower Project, Tanzania

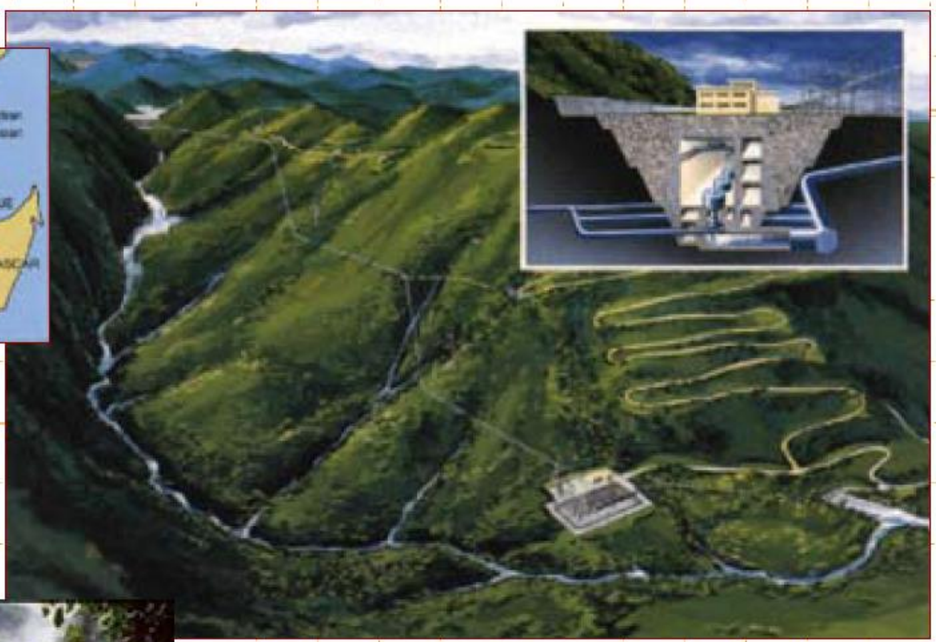

The Lower Kihansi hydroelectric project seeks to utilise the waters of the Kihansi river by channelling part of the river flow upstream of the Kihansi Falls into an inclined high pressure headrace tunnel. The headrace tunnel was planned to be largely unlined.

Unlined tunnels cost 3 to 5 times less than lined tunnels; in this case a cost savings on the order of $10-15 million.

Lower Kihansi Hydropower Project, Tanzania

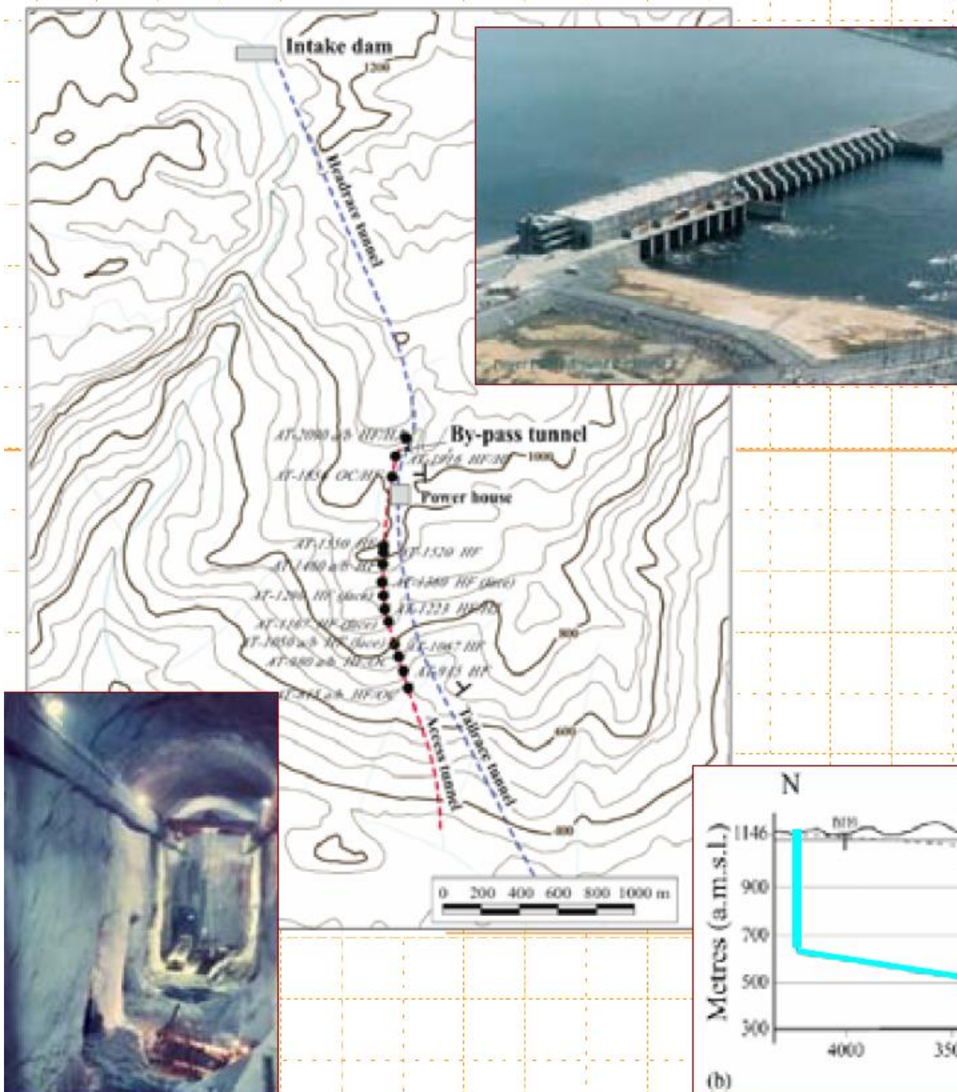

To permit this, the minimum principal stress along the tunnel trajectory under operational conditions would have to be at least equal to the water head times a 1.2 safety factor.

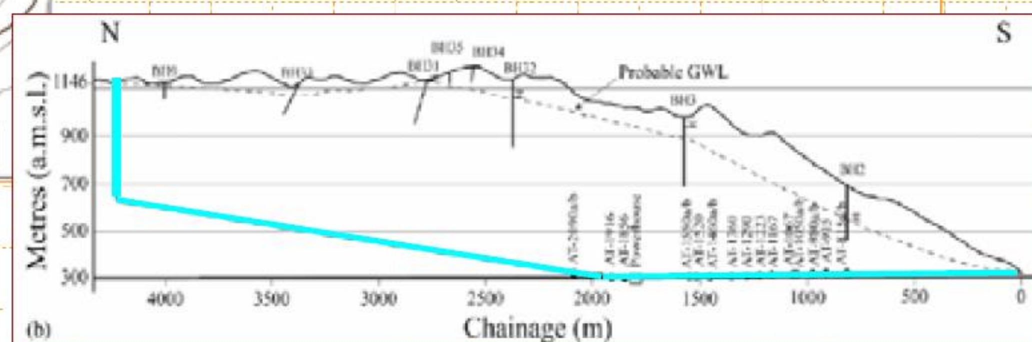

Dahlø *et al.* (2003)

Why Study Stress?

Stress is a concept which is fundamental to rock mechanics principles and applications. There are three basic reasons to understand stress in the context of engineering rock mechanics:

- There is a pre-existing stress state in the ground and we need to understand it, both directly and as the stress state applies to analysis and design.
- During rock excavation, the stress state can change dramatically. This is because rock, which previously contained stresses, has been removed and the loads must be redistributed.
- Stress is not familiar: it is a tensor quantity and tensors are not encountered in everyday life.

Why Determine *In Situ* Stress?

The basic motivations for *in situ* stress determination are two-fold:

- Engineering analyses require boundary conditions. One of the most important boundary conditions for the analysis of underground excavations is *in-situ* stress.

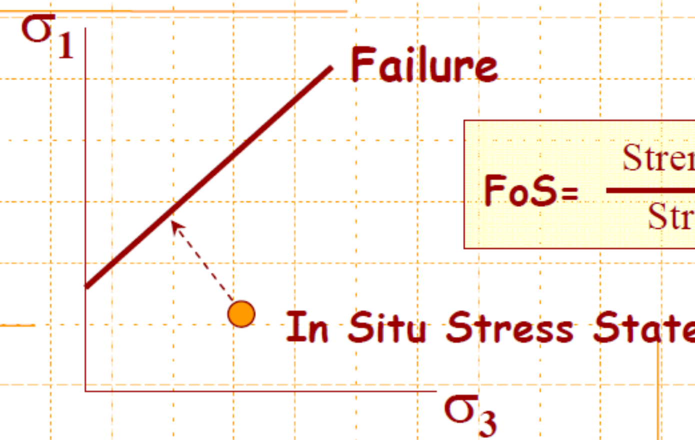

$$\text{FoS} = \frac{\text{Strength}}{\text{Stress}}$$

- To have a basic knowledge of the stress state (e.g. the direction and magnitude of the major principal stress; the direction in which the rock is most likely to fail; etc.).

Civil and mining engineering
- Stability of underground excavations
- Drilling and blasting
- Pillar design
- Design of support systems
- Prediction of rock bursts
- Fluid flow and contaminant transport
- Dams
- Slope stability

Geology/geophysics
- Earthquake prediction
- Plate tectonics
- Neotectonics
- Structural geology

Energy development
- Borehole stability and deviation
- Fracturing and fracture propagation
- Fluid flow and geothermal problems
- Reservoir production management
- Energy extraction and storage

Presentation of In Situ Stress Data

The stress state at a point in a rock mass is generally presented in terms of the magnitude and orientation of the principal stresses (remember that the stress state is completely described by six parameters).

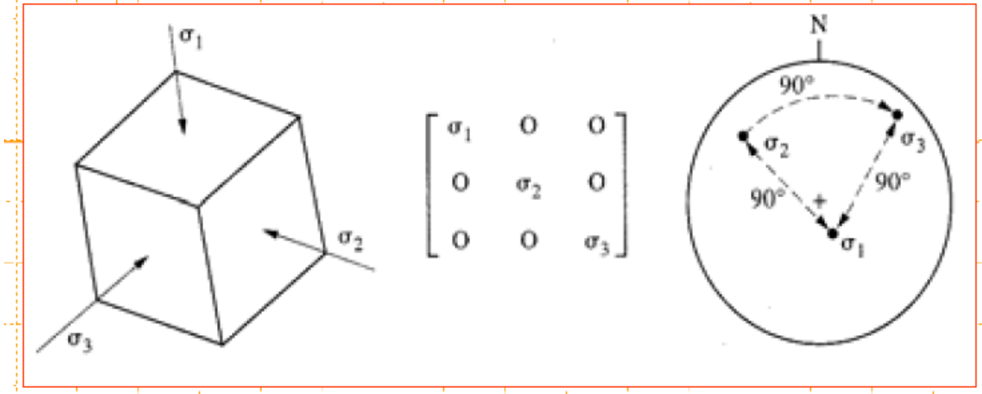

Stress	(MPa)	Trend (°)	Plunge (°)
Sigma 1	10	210	70
Sigma 2	8	320	10
Sigma 3	5	50	15

… principal stresses acting on a cube (left), expressed in matrix form (centre), and shown on a hemispherical projection in terms of their orientation.

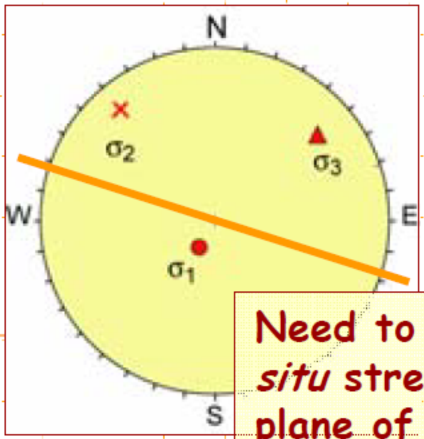

Need to know the *in-situ* stress in the plane of a tunnel for plane strain analysis.

In Situ Stress

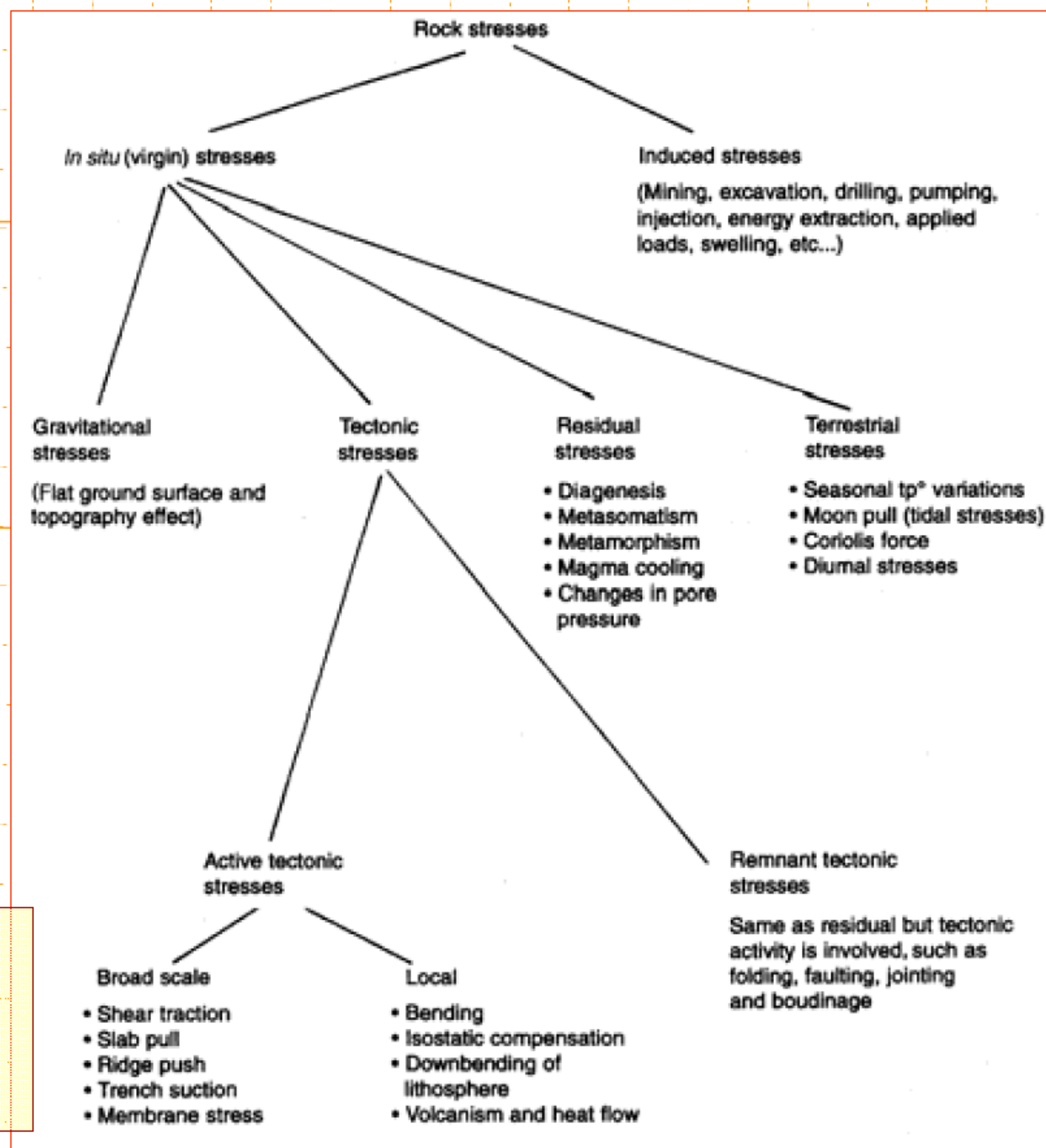

Amadei & Stephansson (1997)

… components of rock stress and stress terminology.

In Situ Stress

When considering the loading conditions imposed on the rock mass, it must be recognized that an *in situ* pre-existing state of stress already exists in the rock.

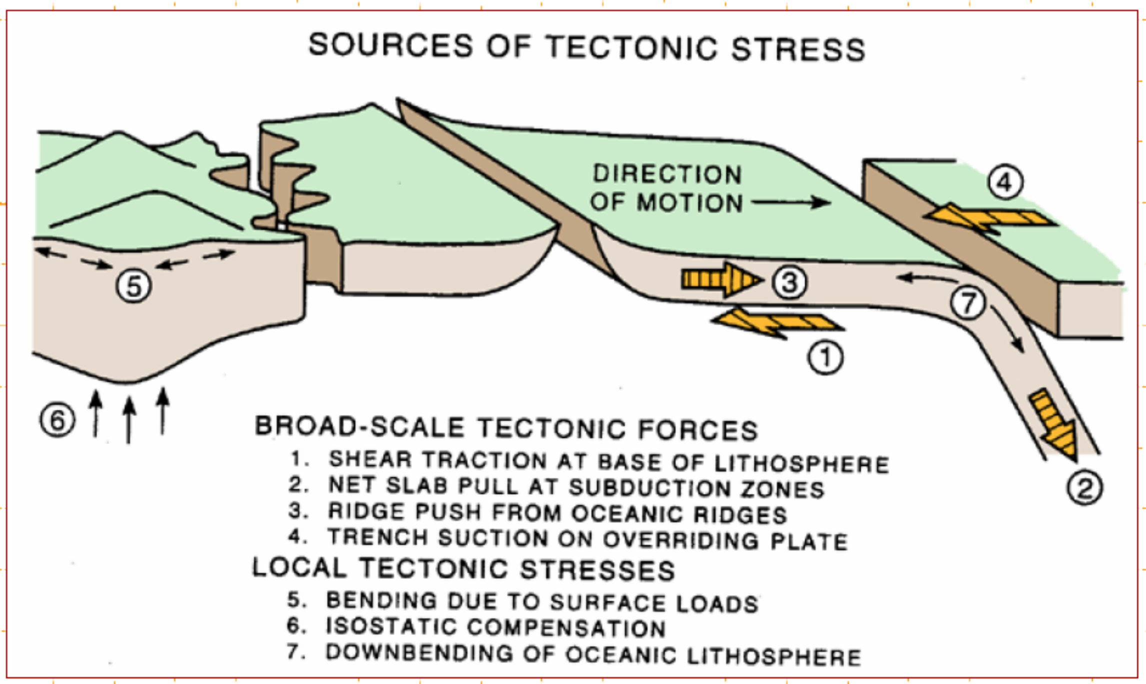

Zoback *et al.* (1989)

… forces responsible for tectonic stresses.

Estimation of *In Situ* Stresses - Vertical

As a first approximation, the principal *in situ* stresses can be assumed to act vertically (one component) and horizontally (two components).

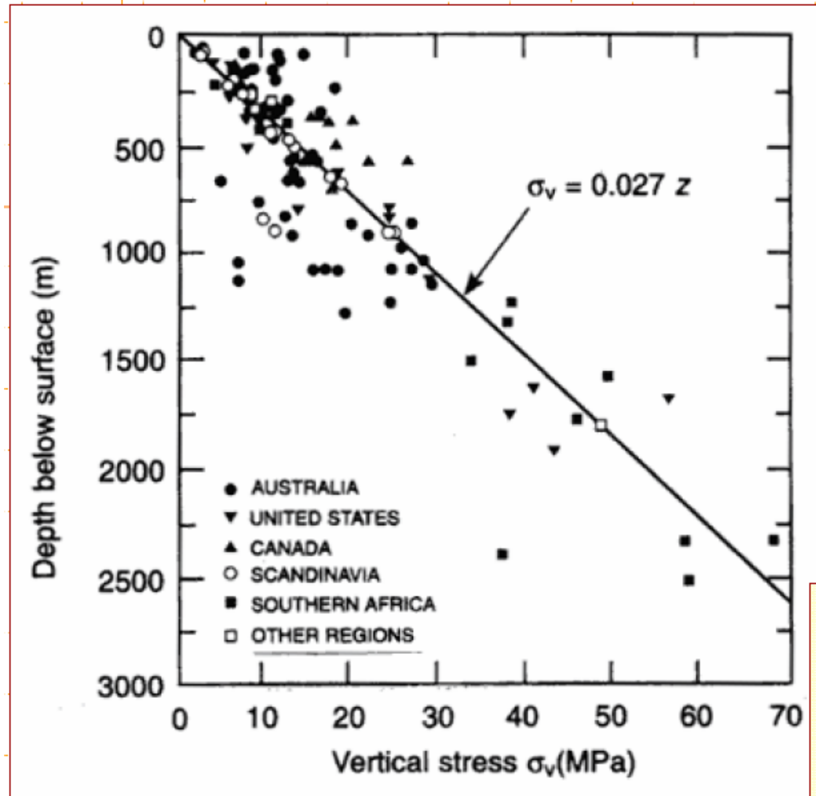

Hoek & Brown (1980)

The vertical stress component is assumed to increase with depth due to the weight of the overburden:

$$\sigma_v = \gamma z$$

Where z is the depth, measured in metres below ground surface and γ is the unit weight, measured in MN/m^3.

As a rule of thumb, taking the average density of rock into account, 40 m of overlying rock induces 1 MPa stress.

Estimation of *In Situ* Stresses - Horizontal

The horizontal stress can be estimated using of elastic theory. If we consider the strain along any axis of a small cube at depth, then the total strain can be found from the strain due to the axial stress, subtracting the strain components due to the two perpendicular stresses.

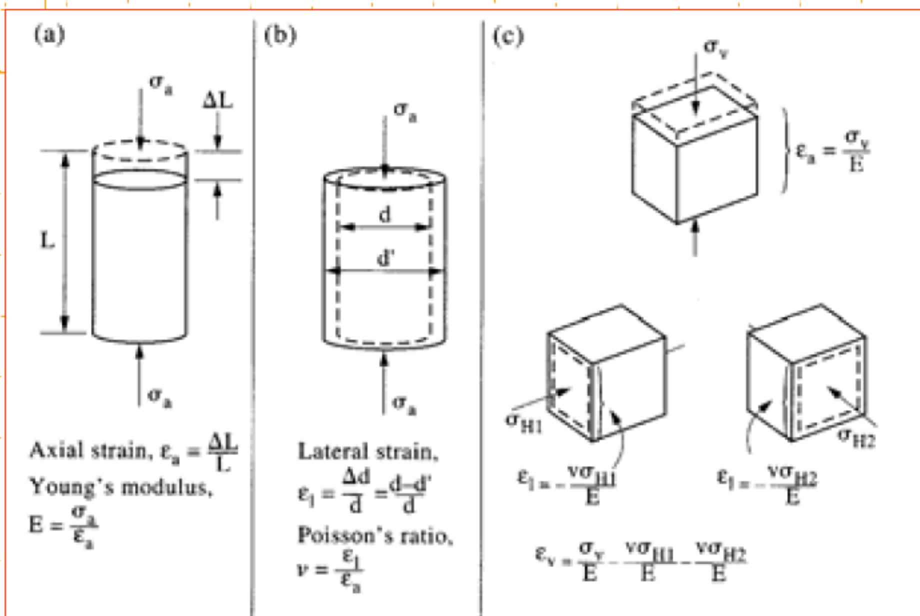

Hudson & Harrison (1997)

For example:

$$\varepsilon_V = \frac{\sigma_V}{E} - \frac{\nu\sigma_{H1}}{E} - \frac{\nu\sigma_{H2}}{E}$$

$$\varepsilon_{H1} = \frac{\sigma_{H1}}{E} - \frac{\nu\sigma_{H2}}{E} - \frac{\nu\sigma_V}{E}$$

In Situ Stresses & Geological Structure

Discontinuities, e.g. fault zones, act to dramatically perturb the stress field and thus the magnitudes and orientations of the principal stresses. This may lead to bias if the stress measurements are made near an isolated fracture.

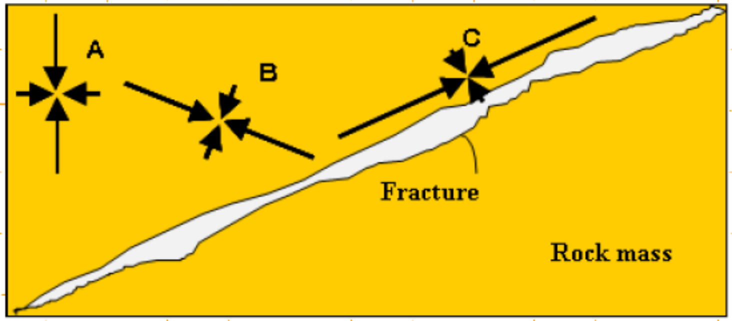

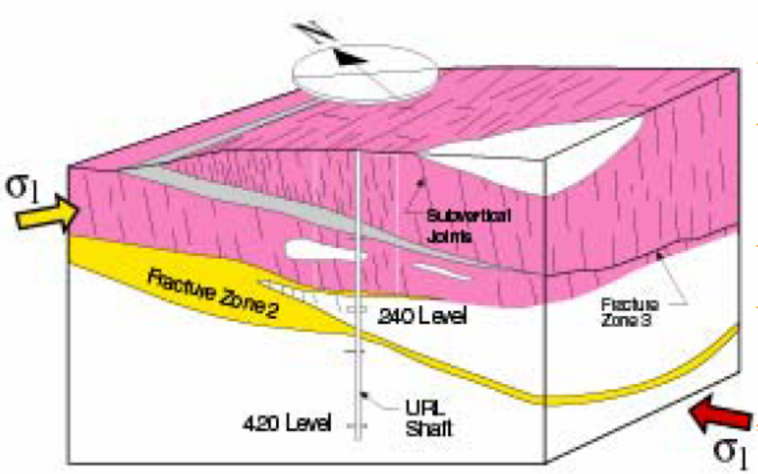

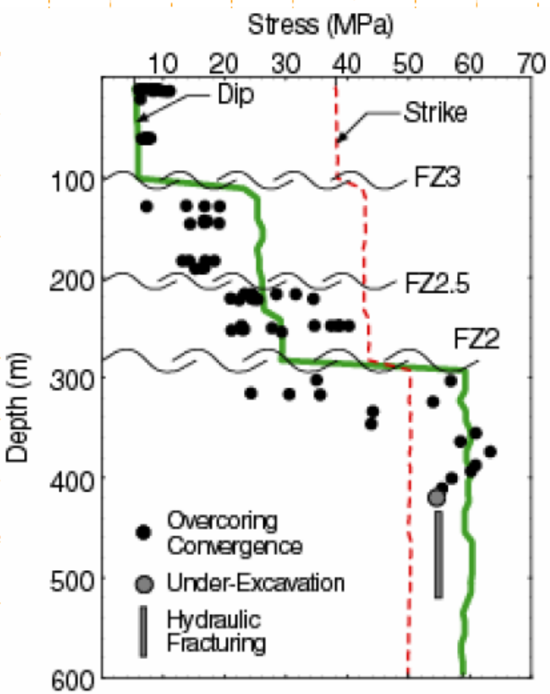

Martin & Chandler (1993)

Reasons for High Horizontal Stresses

High horizontal stresses are caused by factors relating to erosion, tectonics, rock anisotropy, local effects near discontinuities, and scale effects:

Erosion – if horizontal stresses become 'locked in', then the erosion/removal of overburden (i.e. decrease in σ_V) will result in an increase in K ratio (σ_H/σ_V).

Tectonics – different forms of tectonic activity (e.g. subduction zones), can produce high horizontal stresses.

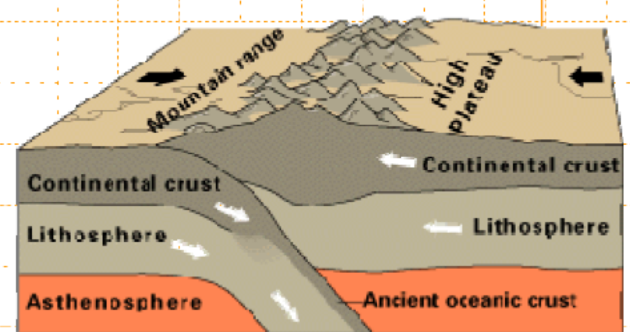

Continental-continental convergence

Methods of Stress Determination

Any system utilized for estimating *in situ* stresses should involve a minimum of six independent measurements. Accordingly, there are methods of 'direct' stress measurement and there are methods of estimating the stresses via 'indirect' or 'indicator' methods.

	Method	*Volume (m^3)*
Hydraulic methods	Hydraulic fracturing	0.5–50
	Sleeve fracturing	10^{-2}
	Hydraulic tests on pre-existing fractures (HTPF)	1–10
Relief methods	Surface relief methods	1–2
	Undercoring	10^{-3}
	Borehole relief methods (overcoring, borehole slotting, etc.)	10^{-3}–10^{-2}
	Relief of large rock volumes (bored raise, under-excavation technique, etc.)	10^{2}–10^{3}
Jacking methods	Flat jack method	0.5–2
	Curved jack method	10^{-2}
Strain recovery methods	Anelastic strain recovery (ASR)	10^{-3}
	Differential strain curve analysis (DSCA)	10^{-4}
Borehole breakout method	Caliper and dipmeter analysis	10^{-2}–10^{2}
	Borehole televiewer analysis	10^{-2}–10^{2}
Other methods	Fault slip data analysis	10^{8}
	Earthquake focal mechanisms	10^{9}
	Indirect methods (Kaiser effect, etc.)	10^{-4}–10^{-3}
	Inclusions in time-dependent rock	10^{-2}–1
	Measurement of residual stresses	10^{-5}–10^{-3}

Amadei & Stephansson (1997)

Indicator Methods of Stress Determination

By careful study of earthquake waves recorded by seismographs, it is possible to tell the direction of motion of the fault that caused the earthquake.

By analyzing the earthquake fault-plane solution (i.e. focal mechanism), a best fit regional stress tensor can be determined by means of an inversion technique.

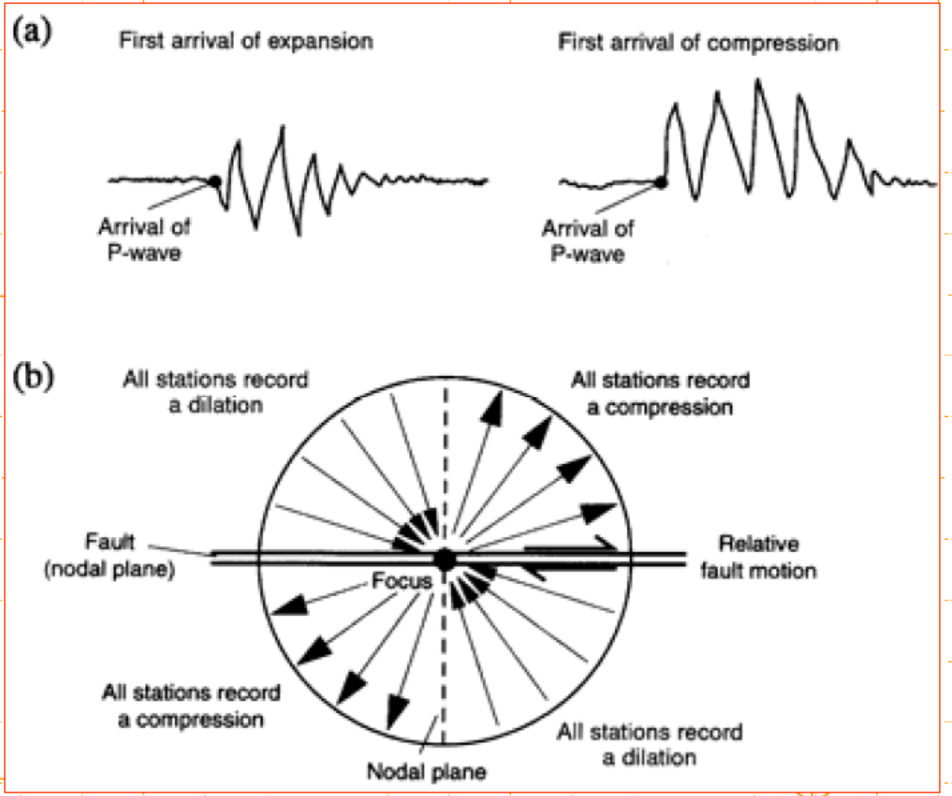

Amadei & Stephansson (1997)

Indicator Methods of Stress Determination

The rock around a circular excavation may not be able to sustain the compressive stress concentration induced during excavation. Failure of the rock results in zones of enlargement called 'breakouts'. There is experimental evidence that breakouts occur in the direction parallel to the minimum *in situ* stress component.

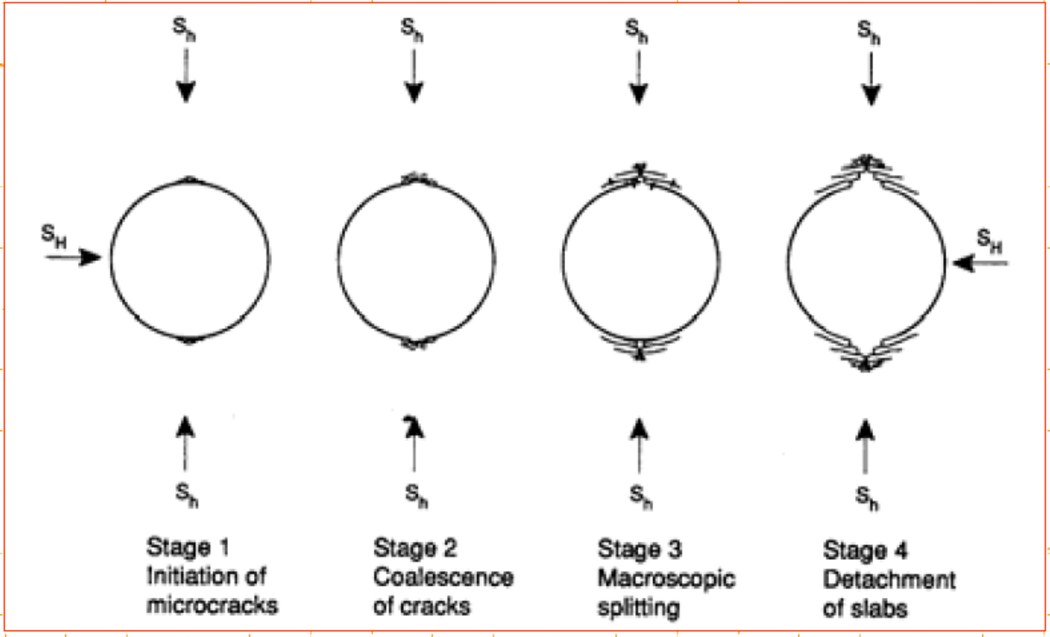

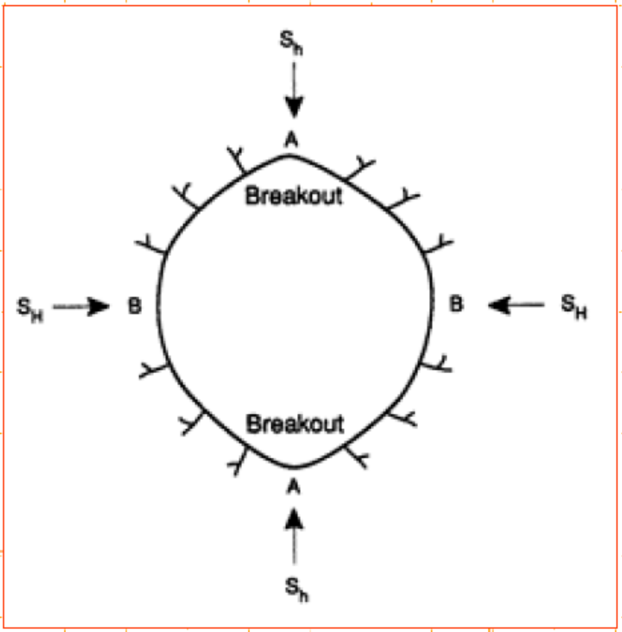

Amadei & Stephansson (1997)

Indicator Methods of Stress Determination

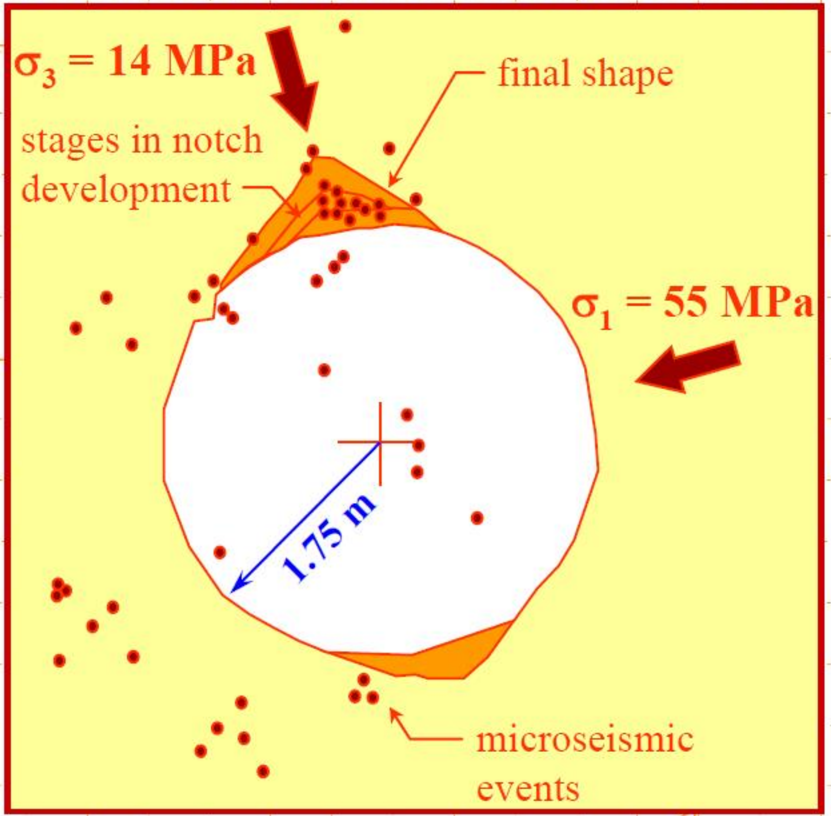

… stress-controlled tunnel breakout at the URL in Canada.

Methods of Stress Determination

1. Flatjack

$$\begin{bmatrix} \sigma_{xx} & \tau_{xy} & \tau_{xz} \\ & \sigma_{yy} & \tau_{yz} \\ \text{Symm.} & & \sigma_{zz} \end{bmatrix}$$

One normal stress component determined, say parallel to x-axis.

2. Hydraulic fracturing

$$\begin{bmatrix} \sigma_1 & 0 & 0 \\ & \sigma_2 & 0 \\ \text{Symm.} & & \sigma_3 \end{bmatrix}$$

Principal stresses assumed parallel to axes i.e. plane of the fracture, two determined, say σ_1 and σ_3, one estimated, say σ_2.

3. USBM overcoring torpedo

$$\begin{bmatrix} \sigma_{xx} & \tau_{xy} & \tau_{xz} \\ & \sigma_{yy} & \tau_{yz} \\ \text{Symm.} & & \sigma_{zz} \end{bmatrix}$$

Three components in 2-D determined from three measurements of borehole diameter change.

4. CSIRO overcoring gauge

$$\begin{bmatrix} \sigma_{xx} & \tau_{xy} & \tau_{xz} \\ & \sigma_{yy} & \tau_{yz} \\ \text{Symm.} & & \sigma_{zz} \end{bmatrix}$$

All six components determined from six (or more) measurements of strain at one time.

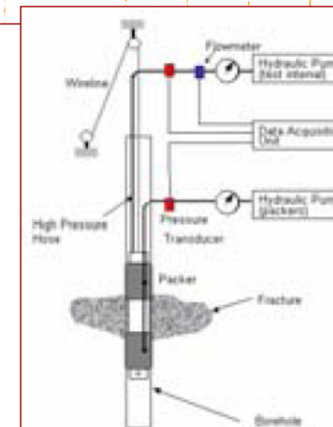

Hudson & Harrison (1997)

... the four ISRM suggested methods for rock stress determination and their ability to determine the 6 independent components of the stress tensor over one test/application of the particular method.

Flatjack Method

A flatjack is comprised of two metal sheets placed together and welded around their periphery. A feeder tube inserted in the middle allows the flatjack to be pressurized with oil or water.

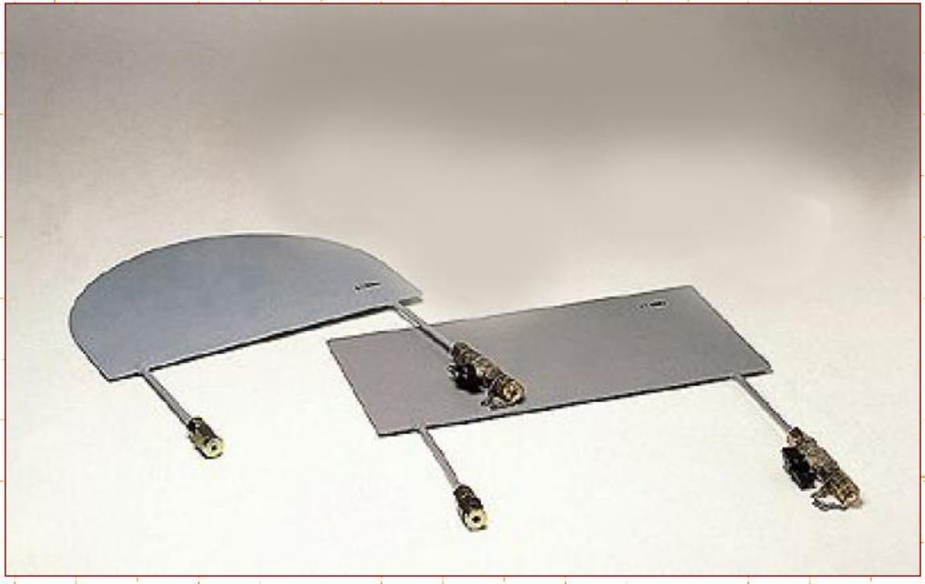

Flatjack Method

The flatjack method involves the placement of two pins fixed into the wall of an excavation. The distance, *d*, is then measured accurately. A slot is cut into the rock between the pins. If the normal stress is compressive, the pins will move together as the slot is cut. The flatjack is then placed and grouted into the slot.

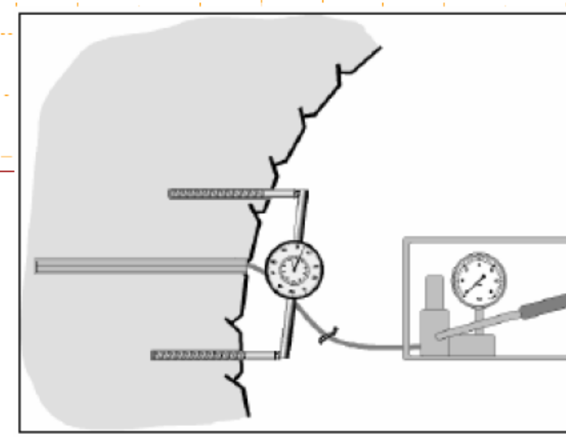

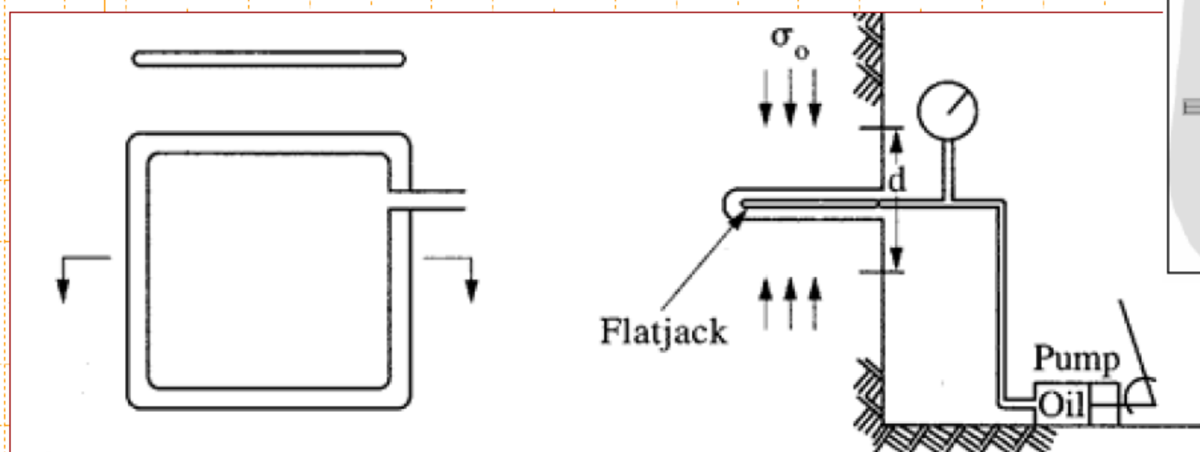

Flatjack Method

On pressurizing the flatjack, the pins will move apart. It is assumed that, when the pin separation distance reaches the value it had before the slot was cut, the force exerted by the flatjack on the walls of the slot is the same as that exerted by the pre-existing normal stress.

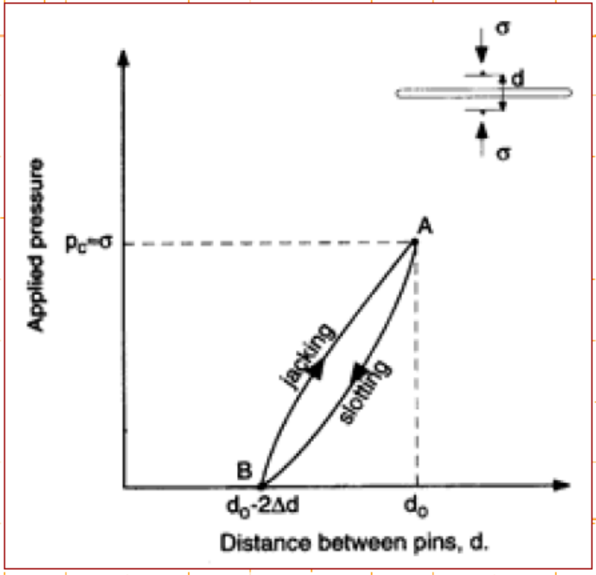

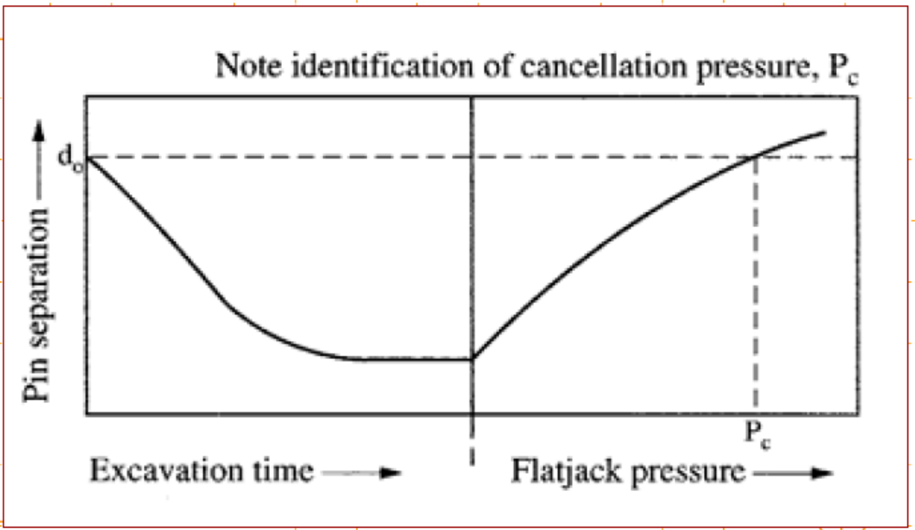

Hudson & Harrison (1997)

Flatjack Method

The major disadvantage with the system is that the necessary minimum number of 6 tests, at different orientations, have to be conducted at 6 different locations and it is therefore necessary to distribute these around the boundary walls of an excavation.

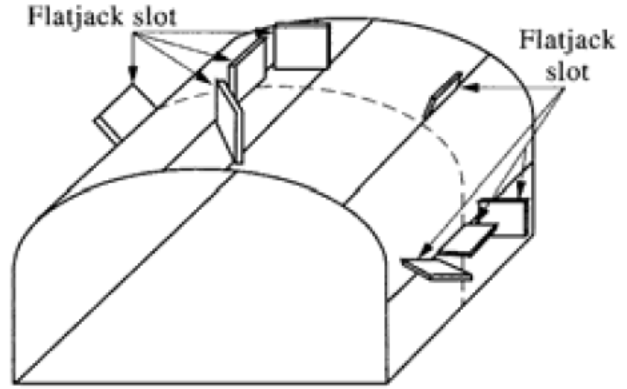

1. **Flatjack**

$$\begin{bmatrix} \sigma_{xx} & \tau_{xy} & \tau_{xz} \\ & \sigma_{yy} & \tau_{yz} \\ \text{Symm.} & & \sigma_{zz} \end{bmatrix}$$

One normal stress component determined, say parallel to x-axis.

Hudson & Harrison (1997)

It is also important to note that the excavation from which the tests are made will disturb the pre-existing stress state, and so the new redistribution of stresses should be accounted for.

Hydraulic Fracturing Method

The hydraulic fracturing method involves the pressuring of a borehole interval, typically 1 m long, isolated using a straddle packer system. The isolated zone is pressurized by water until a fracture occurs in the rock.

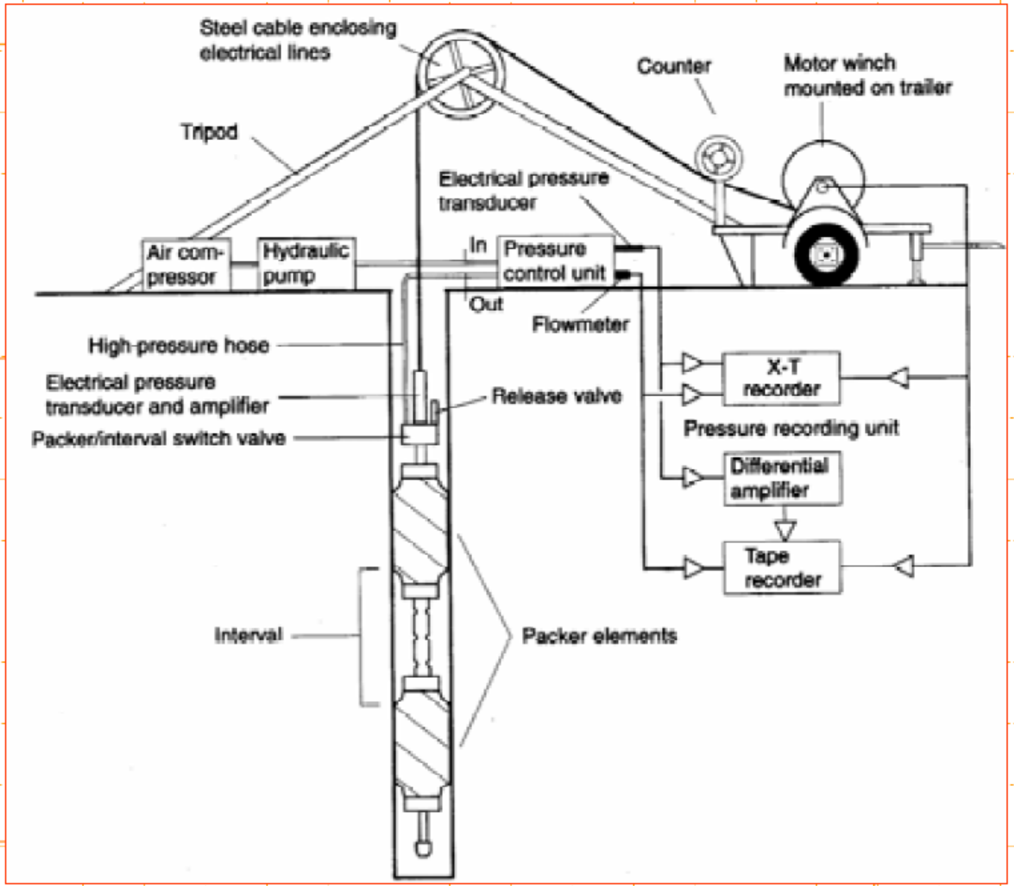

Amadei & Stephansson (1997)

Hydraulic Fracturing Method

The two measurements taken are the water pressure when the fracture occurs and the subsequent pressure required to hold the fracture open. These are referred to as the breakdown pressure (P_c' or P_B) and the shut-in pressure (P_s).

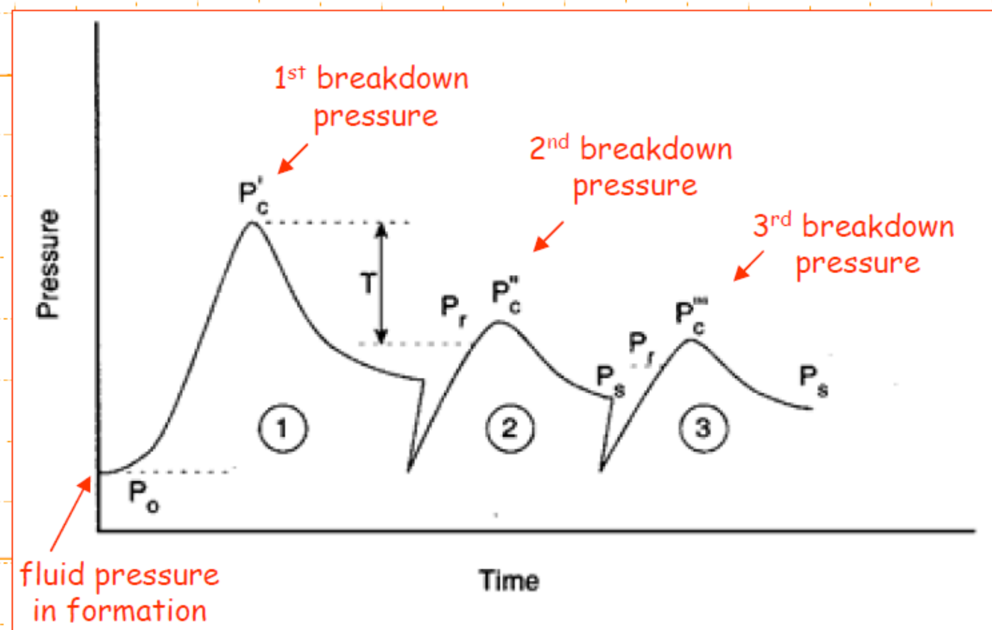

Amadei & Stephansson (1997)

Hydraulic Fracturing Method

In calculating the *in* situ stresses, the shut-in pressure (P_s) is assumed to be equal to the minor horizontal stress, σ_h.

The major horizontal stress, σ_H, is then found from the breakdown pressure (P_c' or P_B). In this calculation, the breakdown pressure has to overcome the minor horizontal principal stress (concentrated three times by the presence of the borehole) and overcome the *in situ* tensile strength of the rock; it is assisted by the tensile component of the major horizontal principal stress.

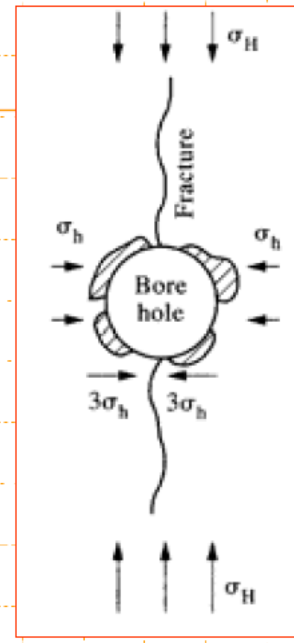

Relationships

$\sigma_h = P_s$

$\sigma_H = 3\sigma_h - P_c' - P_o + \sigma_t$

$\sigma_t = P_c' - P_r$

$\sigma_H = 3\sigma_h - P_r - P_o$

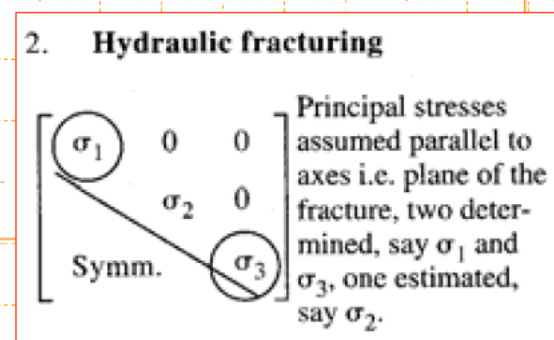

Hudson & Harrison (1997)

Hydraulic Fracturing Method

The analysis assumes that the induced fracture has propagated in a direction perpendicular to the minor principal stress.

Other assumptions include that of elasticity in the rock forming the borehole wall (from which the borehole stress concentration factor of three is derived), and impermeability of the host rock so that pumped water has not significantly penetrated the rock and affected the stress distribution.

The tensile strength of the rock can be obtained from test performed by pressurizing hollow rock cylinders.

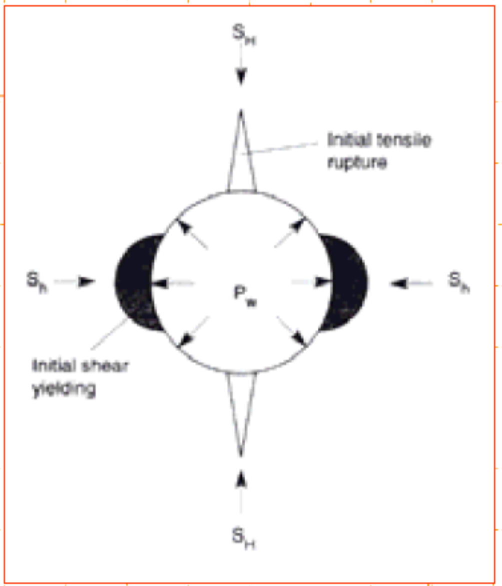

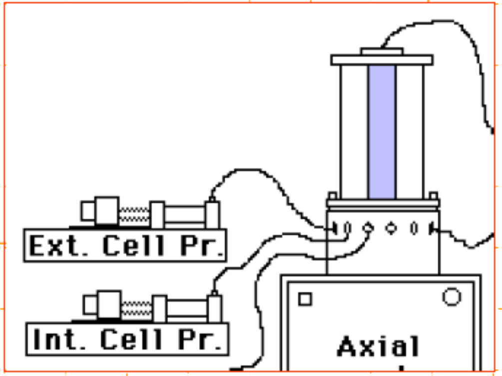

Hydraulic Fracturing Method

There are also several problems inherent in the use of this equipment to measure the stress state. For example, it can often be difficult, if not impossible, to identify a 1 m length of borehole which is fracture free.

Furthermore, there can be difficulties measuring water pressures accurately, and in correctly identifying the breakdown and shut-in pressures.

Lastly, it is often a completely unjustified assumption that the borehole is indeed parallel to a principal stress, and sometimes, that the vertical stress can be calculated from the depth of overburden.

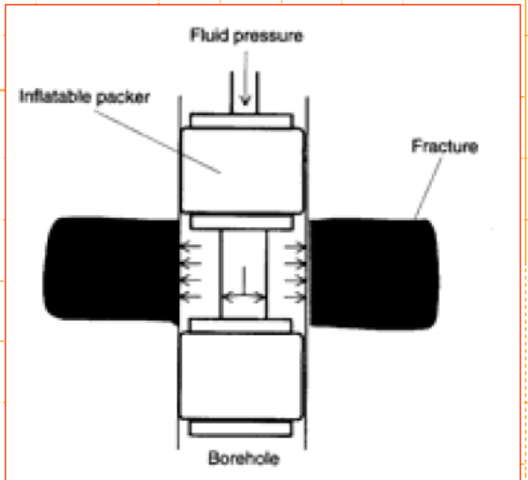

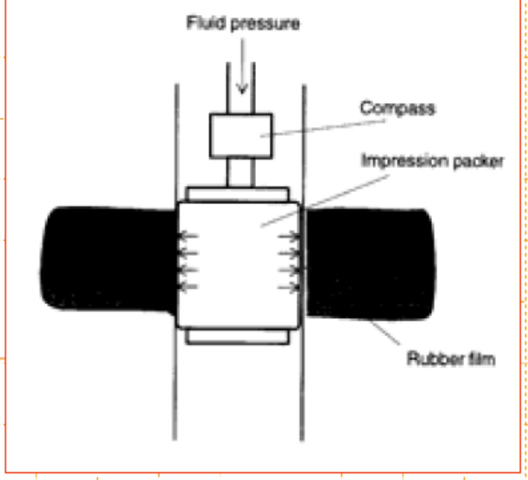

Hydraulic Fracturing Method - HTPF

The HTPF method (Hydraulic Testing on Pre-existing Fractures), consists of reopening an existing fracture of known orientation that has previously been isolated in between two packers. By using a low fluid injection rate, the fluid pressure which balances exactly the normal stress across the fracture is measured.

The method is then repeated for other non-parallel fractures of known orientation.

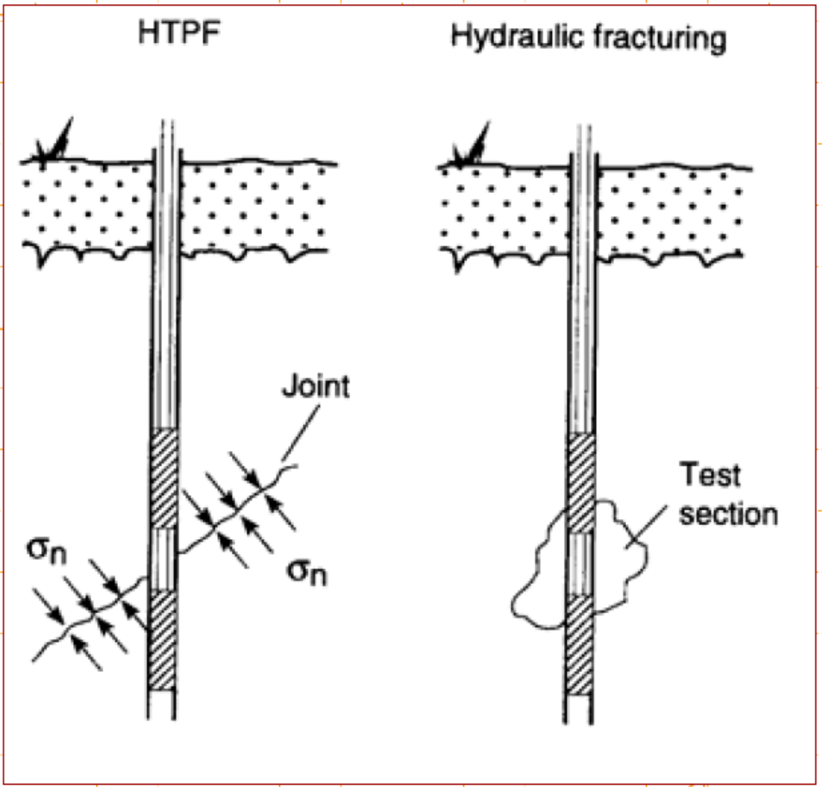

Amadei & Stephansson (1997)

Hydraulic Fracturing Method - HTPF

By determining the normal stresses acting across several non-parallel fractures and knowing their orientation, a system of equations can be created to determine the six *in situ* stress components without making any assumption with regards to the orientation of the principal stresses and the rock's constitutive behaviour.

It is the only hydraulic method that does not have to assume that the principal stress directions are aligned vertically and horizontally.

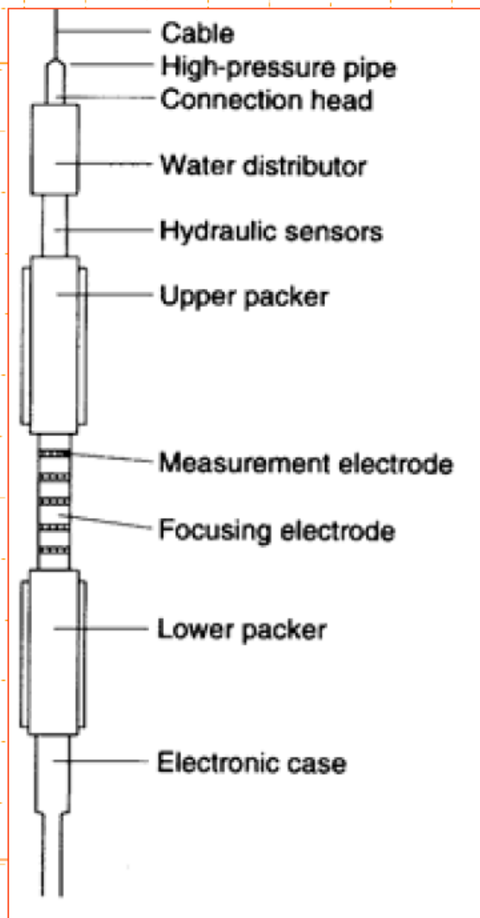

Hydraulic Fracturing Method - Example

Q. A hydraulic fracture test in a granite rock mass yield the following results:

Depth (m)	Breakdown pressure, P_B (MPa)	Shut-in pressure, P_S (MPa)
500	14.0	8.0

Given that the tensile strength of the rock is 10 MPa, estimate the values of σ_1, σ_2 and σ_3 assuming that one principal stress is vertical and that the pressure values were adjusted to account for the formation pressures (i.e. P_o=0 for calculation purposes).

A. Assuming that the rock mass was behaving as an elastic material,

Relationships

$\sigma_h = P_s$

$\sigma_H = 3\sigma_h - P_c' - P_o + \sigma_t$

$\sigma_t = P_c' - P_r$

$\sigma_H = 3\sigma_h - P_r - P_o$

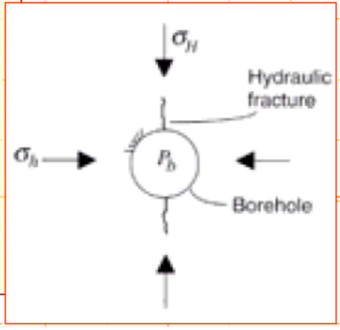

The minimum horizontal stress can be calculated from the expression:

$\sigma_h = P_s$

$\sigma_h = 8$ MPa

Hydraulic Fracturing Method - Example

Q. A hydraulic fracture test in a granite rock mass yield the following results:

Depth (m)	Breakdown pressure, P_B (MPa)	Shut-in pressure, P_S (MPa)
500	14.0	8.0

Given that the tensile strength of the rock is 10 MPa, estimate the values of σ_1, σ_2 and σ_3 assuming that one principal stress is vertical and that the pressure values were adjusted to account for the formation pressures (i.e. P_o=0 for calculation purposes).

A. The maximum horizontal stress can be calculated from the expression:

$$\sigma_H = 3\sigma_h - P_c' - \cancelto{0}{P_o} + \sigma_t \quad \Rightarrow \quad \sigma_H = 3(8\ \text{MPa}) - 14\ \text{MPa} + 10\ \text{MPa}$$

$$\sigma_H = 20\ \text{MPa}$$

The vertical stress can be estimated from the vertical overburden (assuming a unit weight of 27 kN/m³ for granite):

$$\sigma_V = 500\ \text{m} * 0.0027\ \text{MN/m}^3$$

$$\sigma_V = 13.5\ \text{MPa}$$

$$\boxed{\begin{aligned} \sigma_1 &= \sigma_H = 20\ \text{MPa} \\ \sigma_2 &= \sigma_v = 13.5\ \text{MPa} \\ \sigma_3 &= \sigma_h = 8\ \text{MPa} \end{aligned}}$$

Borehole Relief Methods - Overcoring

The main idea behind relief methods is to isolate (partially or wholly) a rock sample from the stress field that surrounds it and to monitor the response. As such, the stresses are not related to applied pressures, such as with the hydraulic tests. Instead, the stresses are inferred from strains generated by the relief (unloading) process and measured directly on the rock associated with the relief process.

Overcoring methods are by far the most commonly used relief method.

Surface relief methods	• Isolate a block of rock from surrounding rock mass and monitor its surface strain or deformation response: • Monitor hole deformation due to drilling of parallel hole • Center hole drilling or undercoring
Borehole relief methods	• Overcoring of prestressed cells • Overcoring of deformation-type gages such as the USBM gage • Overcoring of a gage attached to the flat end of a borehole: Doorstopper and photoelastic disks • Overcoring of CSIR-type triaxial strain cells • Overcoring of triaxial strain cells attached to the end of a borehole (spherical and conical cells) • Overcoring of stiff, solid or hollow inclusion-type gages • Borehole jack fracturing, or slotting, or deepening • Holographic methods • Undercoring of borehole wall • Borehole tapercoring
Rock mass relief methods	• Bored raise method • Back-analysis • Under-excavation technique

Amadei & Stephansson (1997)

Overcoring Method

Three steps are commonly followed in borehole overcoring:

First, a large diameter borehole is drilled (between 60 and 220 mm) in the volume of rock where the stresses are to be determined. The borehole is drilled to a sufficiently large distance so that stress effects due to any excavations can be neglected.

Second, a small pilot hole (38 mm, sometimes larger) is drilled. The measuring device is then inserted and fastened in this hole.

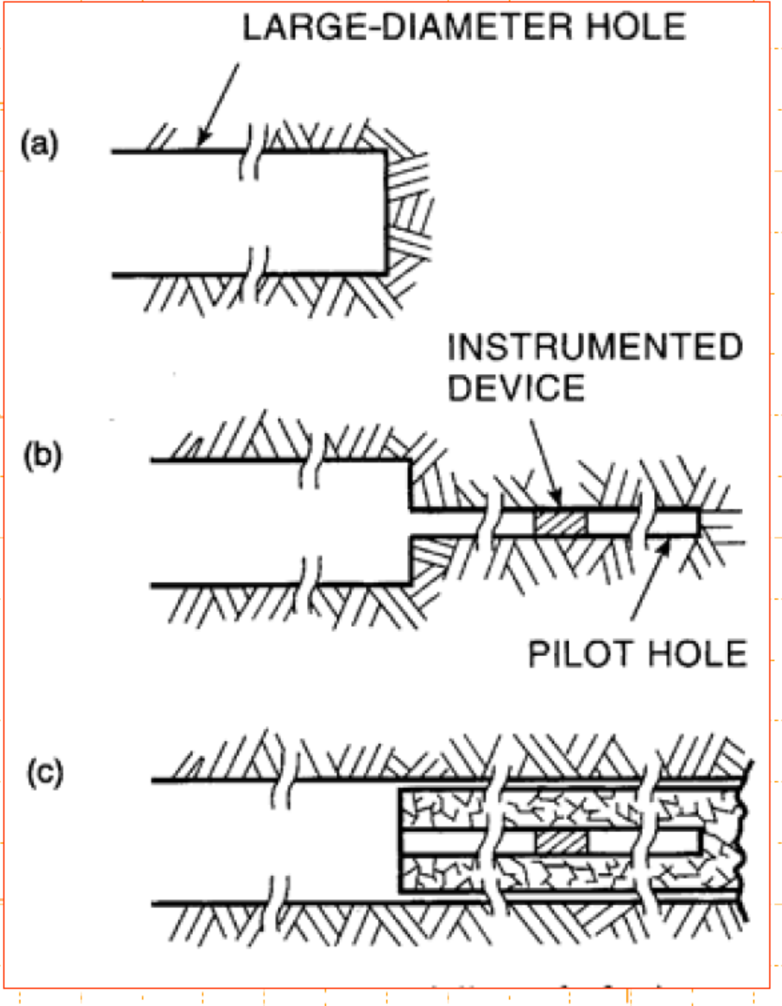

Overcoring Method

Thirdly, the large diameter hole is resumed, relieving stresses and strains in the hollow rock cylinder that is formed. Changes in strain are then recorded with the instrumented device as the overcoring proceeds past the plane of measurement.

Following overcoring, the recovered overcore (containing the instrumented device) is then tested in a biaxial chamber to determine the elastic properties of the rock.

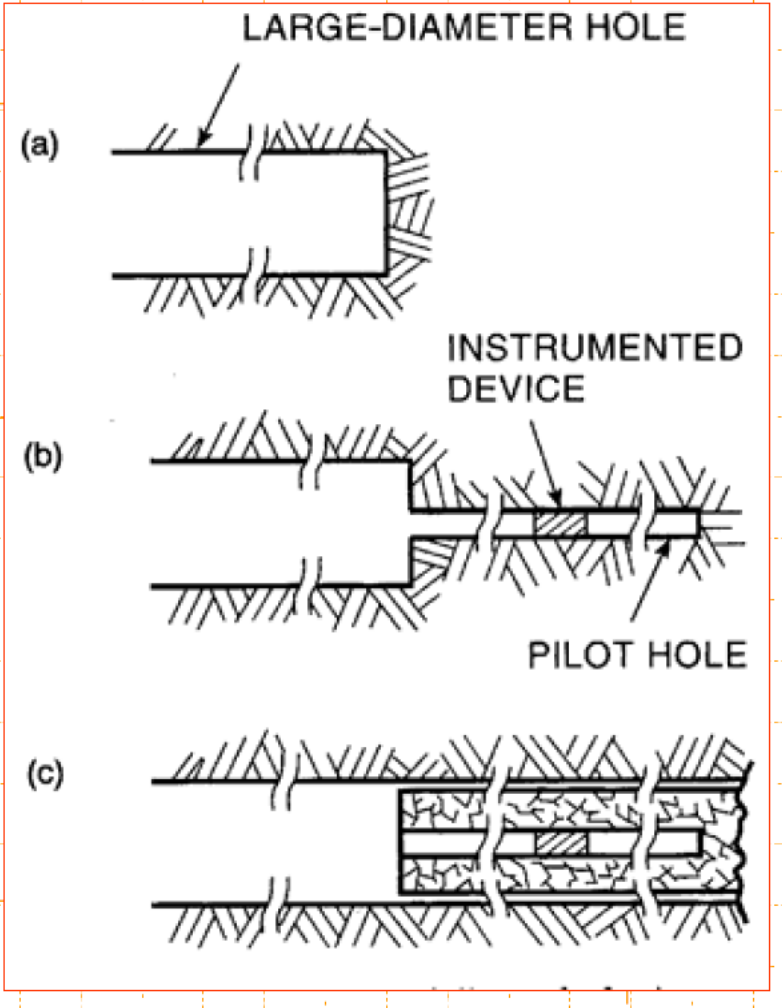

Overcoring Method - USBM Deformation Probe

The USBM technique (from the U.S. Bureau of Mines) allows the complete stress state to be determined from three measurements in boreholes with different orientations when the stresses are released by overcoring the borehole.

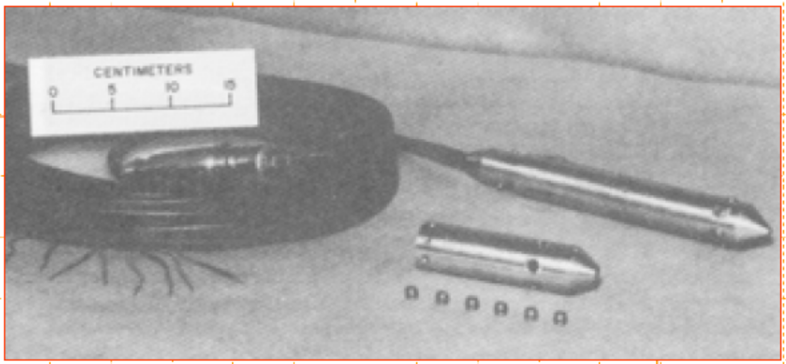

When the probe is inserted in a borehole, six 'buttons' press against the borehole wall and their diametral position is measured by strain gauges bonded to steel cantilevers supporting the buttons.

Overcoring Method – USBM Deformation Probe

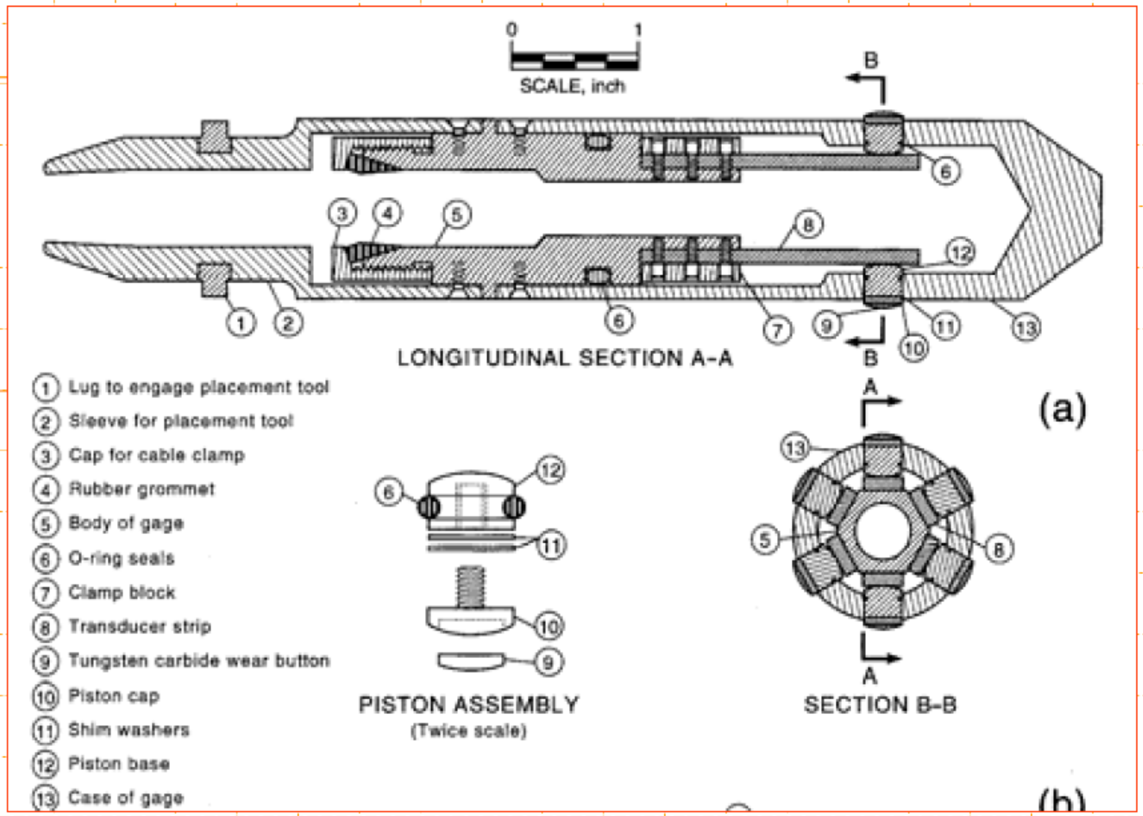

Amadei & Stephansson (1997)

… section through a USBM probe showing cantilevered buttons.

Overcoring Method - USBM

When the borehole is overcored by a larger diameter borehole, the stress state in the resulting hollow cylinder is reduced to zero, the diameter of the hole changes, the buttons move, and hence different strains are induced in the strain gauges.

From these changes, and with the use of elasticity theory, the biaxial stress state in the plane perpendicular to the borehole axis is deduced.

The traces are the electrical output from the device plotted against time during overcoring and hence illustrate the evolution of diametral change during overcoring.

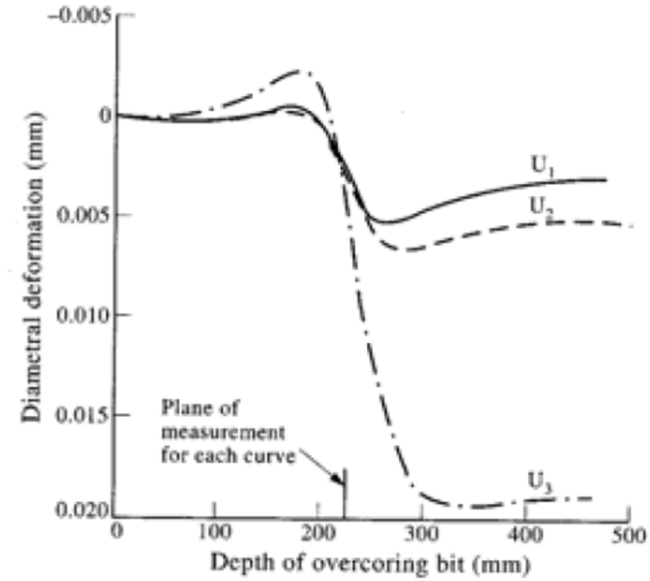

3. USBM overcoring torpedo

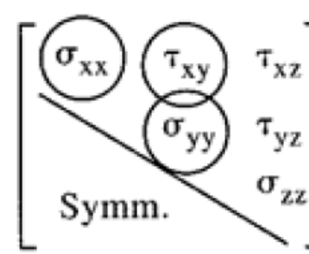

Three components in 2-D determined from three measurements of borehole diameter change.

Overcoring Method - USBM

A useful aspect of this technique is that it produces an annular core which may be used in the laboratory to determine the elastic properties directly.

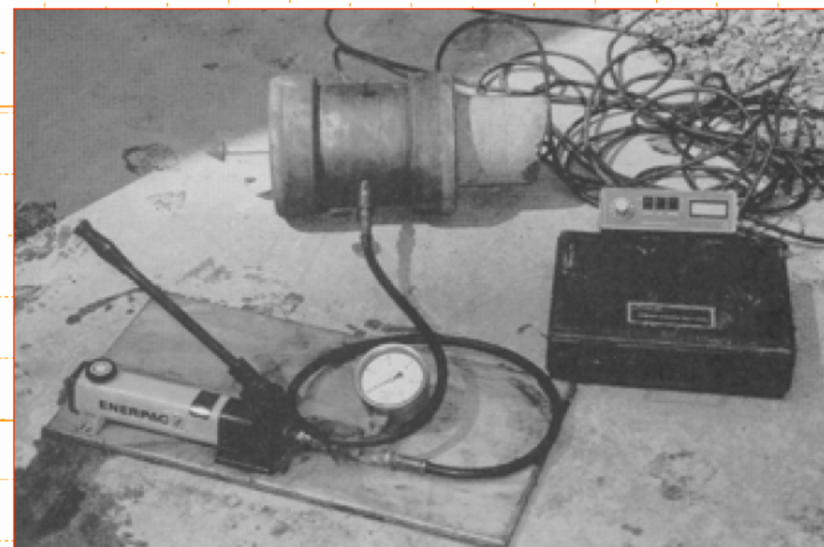

Given the validity of the assumptions, the USBM probe is efficient because it is reusable, permit measurements to be made many times within a borehole and are relatively cheap and robust.

However, the analysis can be complicated by the presence of the borehole, which perturbs the stress state from its natural *in situ* state.

Overcoring Method – CSIRO Hollow Inclusion Cell

The CSIRO device operates on a similar principle to the USBM probe except that it is a gauge which is glued into the borehole and can measure normal strains at a variety of orientations and locations around the borehole wall.

The gauge is glued into position within the pilot hole, initial readings of strain are taken and the gauge is then overcored.

Overcoring Method - CSIRO Hollow Inclusion Cell

Overcoring destresses the resulting hollow cylinder and final strain gauge readings are taken. The gauge has either 9 or 12 separate strain gauges, in rosettes of three, so there is some redundancy in the measurements- thus permitting statistical analysis of the data.

Alternatively, if the rock is assumed to be anisotropic (e.g. transverse isotropic), then the extra readings allow the stress state to be calculated incorporating the rock anisotropy.

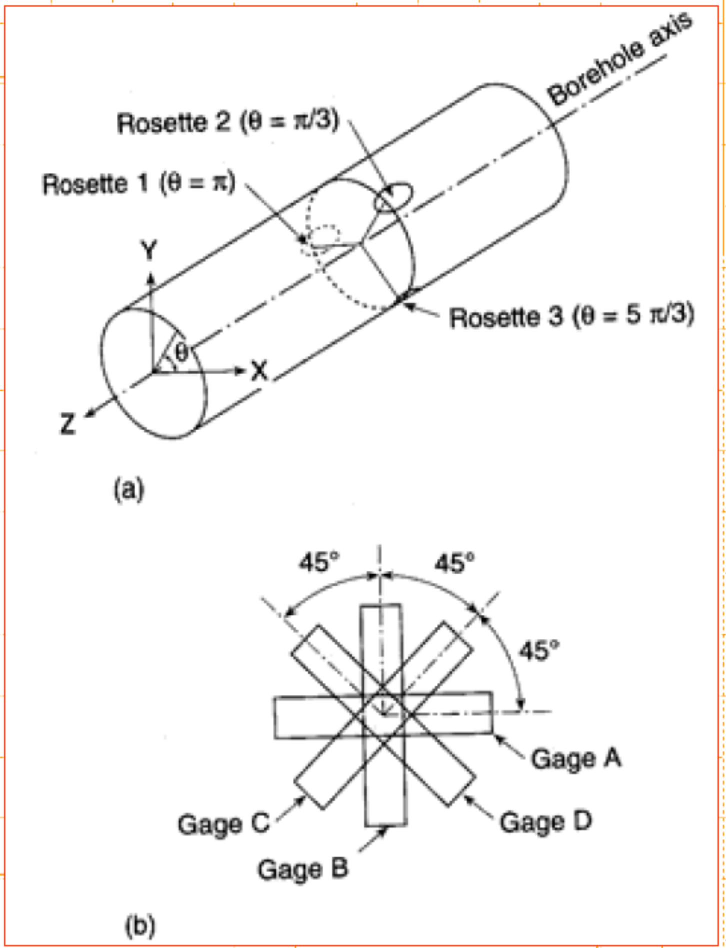

Amadei & Stephansson (1997)

Overcoring Method – CSIRO Hollow Inclusion Cell

The CSIRO measurement cell is one of the few tests that can establish the full stress tensor with one installation.

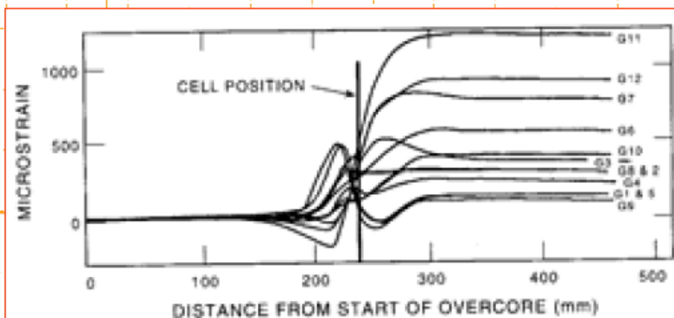

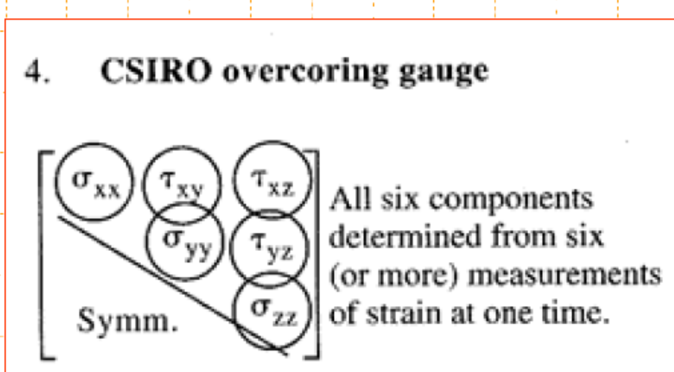

Another advantage of the method is that the hollow rock cylinder can be retrieved and tested under controlled conditions in order to determine the elastic constants and the functionality of the system (e.g. whether strain gauges are properly bonded, whether the test was performed in intact rock, etc.).

One major problem is the environment within the borehole: water or loose material on the borehole walls may hamper bonding of the cell; and drilling fluids may generate temperature effects.

Analysis of induced stresses

When an underground opening is excavated into a stressed rock mass, the stresses in the vicinity of the new opening are re-distributed. Consider the example of the stresses induced in the rock surrounding a horizontal circular tunnel as illustrated in Figure 5, showing a vertical slice normal to the tunnel axis.

new stresses are induced. Three principal stresses σ_1, σ_2 and σ_3 acting on a typical element of rock are shown in Figure 5.

The convention used in rock engineering is that *compressive* stresses are always *positive* and the three principal stresses are numbered such that σ_1 is the largest compressive stress and σ_3 is the smallest compressive stress or the largest tensile stress of the three.

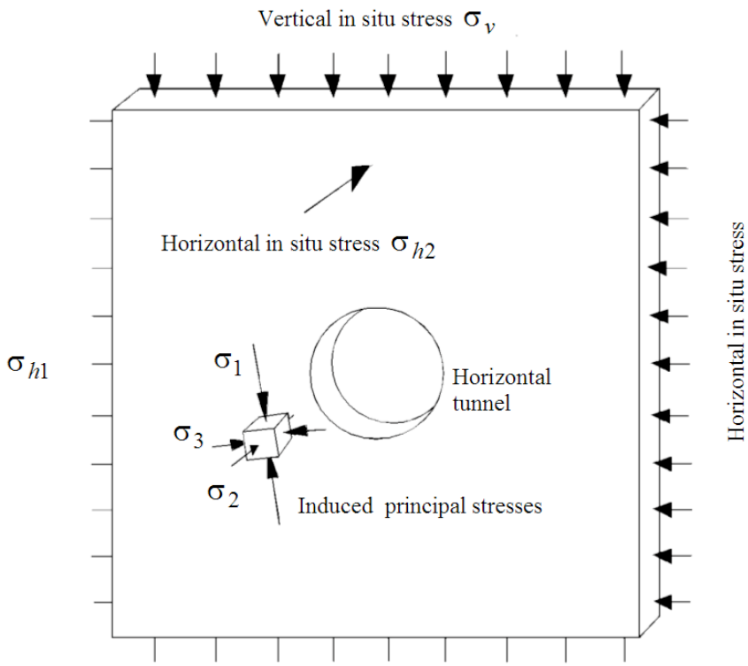

Figure 5: Illustration of principal stresses induced in an element of rock close to a horizontal tunnel subjected to a vertical in situ stress σ_v, a horizontal in situ stress σ_{h1} in a plane normal to the tunnel axis and a horizontal in situ stress σ_{h2} parallel to the tunnel axis.

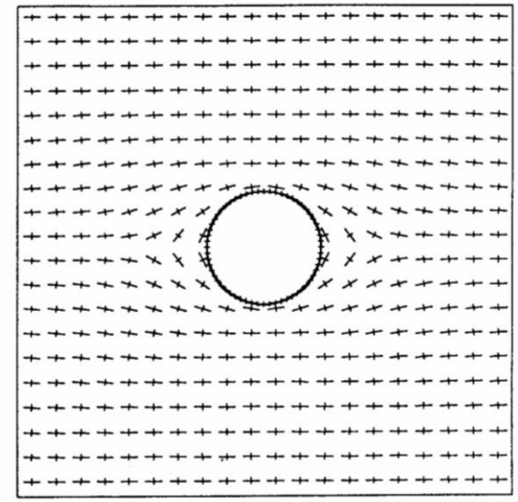

Figure 6: Principal stress directions in the rock surrounding a horizontal tunnel subjected to a horizontal in situ stress σ_{h1} equal to $3\sigma_v$, where σ_v is the vertical in situ stress.

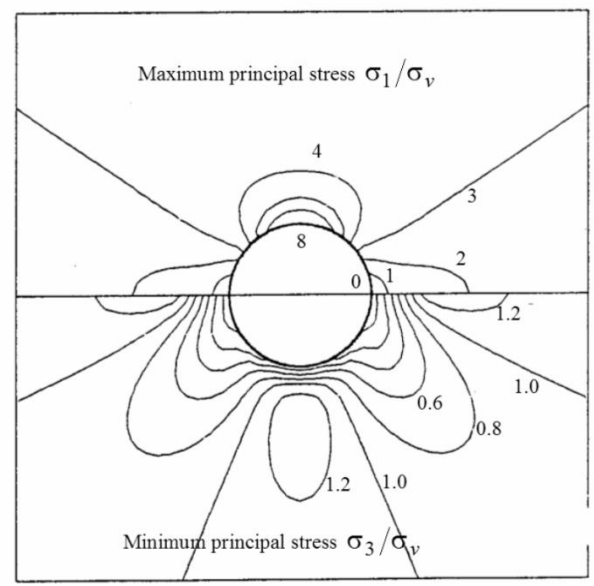

Figure 7: Contours of maximum and minimum principal stress magnitudes in the rock surrounding a horizontal tunnel, subjected to a vertical in situ stress of σ_v and a horizontal in situ stress of $3\sigma_v$.

The three principal stresses are mutually perpendicular but they may be inclined to the direction of the applied in situ stress. This is evident in Figure 6 which shows the directions of the stresses in the rock surrounding a horizontal tunnel subjected to a horizontal in situ stress σ_{h1} equal to three times the vertical in situ stress σ_v. The longer bars in this figure represent the directions of the maximum principal stress σ_1, while the shorter bars give the directions of the minimum principal stress σ_3 at each element considered. In this particular case, σ_2 is coaxial with the in situ stress σ_{h2}, but the other principal stresses σ_1 and σ_3 are inclined to σ_{h1} and σ_v in the immediate vicinity of the tunnel.

Contours of the magnitudes of the maximum principal stress σ_1 and the minimum principal stress σ_3 are given in Figure 7. This figure shows that the redistribution of stresses is concentrated in the rock close to the tunnel and that, at a distance of say three times the radius from the centre of the hole, the disturbance to the in situ stress field is negligible.

An analytical solution for the stress distribution in a stressed elastic plate containing a circular hole was published by Kirsch (1898) and this formed the basis for many early studies of rock behaviour around tunnels and shafts. Following along the path pioneered by Kirsch, researchers such as Love (1927), Muskhelishvili (1953) and Savin (1961) published solutions for excavations of various shapes in elastic plates. A useful summary of these solutions and their application in rock mechanics was published by Brown in an introduction to a volume entitled *Analytical and Computational Methods in Engineering Rock Mechanics* (1987).

Closed form solutions still possess great value for conceptual understanding of behaviour and for the testing and calibration of numerical models. For design purposes, however, these models are restricted to very simple geometries and material models. They are of limited practical value. Fortunately, with the development of computers, many powerful programs that provide numerical solutions to these problems are now readily available. A brief review of some of these numerical solutions is given below.

Numerical methods of stress analysis

Most underground excavations are irregular in shape and are frequently grouped close to other excavations. These groups of excavations can form a set of complex three-dimensional shapes. In addition, because of the presence of geological features such as faults and dykes, the rock properties are seldom uniform within the rock volume of interest. Consequently, closed form solutions are of limited value in calculating the stresses, displacements and failure of the rock mass surrounding underground excavations. A number of computer-based numerical methods have been developed over the past few decades and these methods provide the means for obtaining approximate solutions to these problems.

Numerical methods for the analysis of stress driven problems in rock mechanics can be divided into two classes:

- *Boundary discretization methods*, in which only the boundary of the excavation is divided into elements and the interior of the rock mass is represented mathematically as an infinite continuum. These methods are normally restricted to elastic analyses.
- *Domain discretization methods*, in which the interior of the rock mass is divided into geometrically simple elements each with assumed properties. The collective behaviour and interaction of these simplified elements model the more complex overall behaviour of the rock mass. In other words domain methods allow consideration of more complex material models than boundary methods. *Finite element* and *finite difference* methods are domain techniques which treat the rock mass as a continuum. The *distinct element* method is also a domain method which models each individual block of rock as a unique element.

These two classes of analysis can be combined in the form of *hybrid models* in order to maximise the advantages and minimise the disadvantages of each method.

It is possible to make some general observations about the two types of approaches discussed above. In domain methods, a significant amount of effort is required to create the mesh that is used to divide the rock mass into elements. In the case of complex models, such as those containing multiple openings, meshing can become extremely difficult. In contrast, boundary methods require only that the excavation boundary be discretized and the surrounding rock mass is treated as an infinite continuum. Since fewer elements are required in the boundary method, the demand on computer memory and on the skill and experience of the user is reduced. The availability of highly optimised mesh-generators in many domain models has narrowed this difference to the point where most users of domain programs would be unaware of the mesh generation problems discussed above and hence the choice of models can be based on other considerations.

In the case of domain methods, the outer boundaries of the model must be placed sufficiently far away from the excavations in order that errors, arising from the interaction between these outer boundaries and the excavations, are reduced to an acceptable minimum. On the other hand, since boundary methods treat the rock mass as an infinite continuum, the far field conditions need only be specified as stresses acting on the entire rock mass and no outer boundaries are required. The main strength of boundary methods lies in the simplicity achieved by representing the rock mass as a continuum of infinite extent. It is this representation, however, that makes it difficult to incorporate variable material properties and discontinuities such as joints and faults. While techniques have been developed to allow some boundary element modelling of variable rock properties, these types of problems are more conveniently modelled by domain methods.

Before selecting the appropriate modelling technique for particular types of problems, it is necessary to understand the basic components of each technique.

Boundary Element Method

The boundary element method derives its name from the fact that only the boundaries of the problem geometry are divided into elements. In other words, only the excavation surfaces, the free surface for shallow problems, joint surfaces where joints are considered explicitly and material interfaces for multi-material problems are divided into elements. In fact, several types of boundary element models are collectively referred to as 'the boundary element method' (Crouch and Starfield, 1983). These models may be grouped as follows:

Indirect (Fictitious Stress) method, so named because the first step in the solution is to find a set of fictitious stresses that satisfy prescribed boundary conditions. These stresses are then used in the calculation of actual stresses and displacements in the rock mass.

Direct method, so named because the displacements are solved directly for the specified boundary conditions.

Displacement Discontinuity method, so named because the solution is based on the superposition of the fundamental solution of an elongated slit in an elastic continuum and shearing and normal displacements in the direction of the slit.

The differences between the first two methods are not apparent to the program user. The direct method has certain advantages in terms of program development, as will be discussed later in the section on Hybrid approaches.

The fact that a boundary element model extends 'to infinity' can also be a disadvantage. For example, a heterogeneous rock mass consists of regions of finite, not infinite, extent. Special techniques must be used to handle these situations. Joints are modelled explicitly in the boundary element method using the displacement discontinuity approach, but this can result in a considerable increase in computational effort. Numerical convergence is often found to be a problem for models incorporating many joints. For these reasons, problems, requiring explicit consideration of several joints and/or sophisticated modelling of joint constitutive behaviour, are often better handled by one of the domain methods such as finite elements.

A widely-used application of displacement discontinuity boundary elements is in the modelling of tabular ore bodies. Here, the entire ore seam is represented as a 'discontinuity' which is initially filled with ore. Mining is simulated by reduction of the ore stiffness to zero in those areas where mining has occurred, and the resulting stress redistribution to the surrounding pillars may be examined (Salamon, 1974, von Kimmelmann et al., 1984).

Finite element and finite difference methods

In practice, the finite element method is usually indistinguishable from the finite difference method; thus, they will be treated here as one and the same. For the boundary element method, it was seen that conditions on a domain boundary could be related to the state at *all* points throughout the remaining rock, even to infinity. In comparison, the finite element method relates the conditions at a few points within the rock (nodal points) to the state within a finite closed region formed by these points (the element). In the finite element method the physical problem is modelled numerically by dividing the entire problem region into elements.

The finite element method is well suited to solving problems involving heterogeneous or non-linear material properties, since each element explicitly models the response of its contained material. However, finite elements are not well suited to modelling infinite boundaries, such as occur in underground excavation problems. One technique for handling infinite boundaries is to discretize beyond the zone of influence of the excavation and to apply appropriate boundary conditions to the outer edges. Another approach has been to develop elements for which one edge extends to infinity i.e. so-called 'infinity' finite elements. In practice, efficient pre- and post-processors allow the user to perform parametric analyses and assess the influence of approximated far-field boundary conditions. The time required for this process is negligible compared to the total analysis time.

Joints can be represented explicitly using specific 'joint elements'. Different techniques have been proposed for handling such elements, but no single technique has found universal favour. Joint interfaces may be modelled, using quite general constitutive relations, though possibly at increased computational expense depending on the solution technique.

Once the model has been divided into elements, material properties have been assigned and loads have been prescribed, some technique must be used to redistribute any unbalanced loads and thus determine the solution to the new equilibrium state. Available solution techniques can be broadly divided into two classes - implicit and explicit. Implicit techniques assemble systems of linear equations that are then solved using standard matrix reduction techniques. Any material non-linearity is accounted for by modifying stiffness coefficients (secant approach) and/or by adjusting prescribed variables (initial stress or initial strain approach). These changes are made in an iterative manner such that all constitutive and equilibrium equations are satisfied for the given load state.

The response of a non-linear system generally depends upon the sequence of loading. Thus it is necessary that the load path modelled be representative of the actual load path experienced by the body. This is achieved by breaking the total applied load into load increments, each increment being sufficiently small, so that solution convergence for the increment is achieved after only a few iterations. However, as the system being modelled becomes increasingly non-linear and the load increment represents an ever smaller portion of the total load, the incremental solution technique becomes similar to modelling the quasi-dynamic behaviour of the body, as it responds to gradual application of the total load.

In order to overcome this, a ‘dynamic relaxation’ solution technique was proposed (Otter et al., 1966) and first applied to geomechanics modelling by Cundall (1971). In this technique no matrices are formed. Rather, the solution proceeds explicitly - unbalanced forces, acting at a material integration point, result in acceleration of the mass associated with the point; applying Newton's law of motion expressed as a difference equation yields incremental displacements, applying the appropriate constitutive relation produces the new set of forces, and so on marching in time, for each material integration point in the model. This solution technique has the advantage that both geometric and material non-linearities are accommodated, with relatively little additional computational effort as compared to a corresponding linear analysis, and computational expense increases only linearly with the number of elements used. A further practical advantage lies in the fact that numerical divergence usually results in the model predicting obviously anomalous physical behaviour. Thus, even relatively inexperienced users may recognise numerical divergence.

Most commercially available finite element packages use implicit (i.e. matrix) solution techniques. For linear problems and problems of moderate non-linearity, implicit techniques tend to perform faster than explicit solution techniques. However, as the degree of non-linearity of the system increases, imposed loads must be applied in smaller increments which implies a greater number of matrix re-formations and reductions, and hence increased computational expense. Therefore, highly non-linear problems are best handled by packages using an explicit solution technique.

Distinct Element Method

In ground conditions conventionally described as blocky (i.e. where the spacing of the joints is of the same order of magnitude as the excavation dimensions), intersecting joints form wedges of rock that may be regarded as rigid bodies. That is, these individual pieces of rock may be free to rotate and translate, and the deformation that takes place at block contacts may be significantly greater than the deformation of the intact rock. Hence, individual wedges may be considered rigid. For such conditions it is usually necessary to model many joints explicitly. However, the behaviour of such systems is so highly non-linear, that even a jointed finite element code, employing an explicit solution technique, may perform relatively inefficiently.

An alternative modelling approach is to develop data structures that represent the blocky nature of the system being analysed. Each block is considered a unique free body that may interact at contact locations with surrounding blocks. Contacts may be represented by the overlaps of adjacent blocks, thereby avoiding the necessity of unique joint elements. This has the added advantage that arbitrarily large relative displacements at the contact may occur, a situation not generally tractable in finite element codes.

Due to the high degree of non-linearity of the systems being modelled, explicit solution techniques are favoured for distinct element codes. As is the case for finite element codes employing explicit solution techniques, this permits very general constitutive modelling of joint behaviour with little increase in computational effort and results in computation time being only linearly dependent on the number of elements used. The use of explicit solution techniques places fewer demands on the skills and experience than the use of codes employing implicit solution techniques.

Although the distinct element method has been used most extensively in academic environments to date, it is finding its way into the offices of consultants, planners and designers. Further experience in the application of this powerful modelling tool to practical design situations and subsequent documentation of these case histories is required, so that an understanding may be developed of where, when and how the distinct element method is best applied.

Hybrid approaches

The objective of a hybrid method is to combine the above methods in order to eliminate undesirable characteristics while retaining as many advantages as possible. For example, in modelling an underground excavation, most non-linearity will occur close to the excavation boundary, while the rock mass at some distance will behave in an elastic fashion. Thus, the near-field rock mass might be modelled, using a distinct element or finite element method, which is then linked at its outer limits to a boundary element model, so that the far-field boundary conditions are modelled exactly. In such an approach, the direct boundary element technique is favoured as it results in increased programming and solution efficiency.

Lorig and Brady (1984) used a hybrid model consisting of a discrete element model for the near field and a boundary element model for the far field in a rock mass surrounding a circular tunnel.

Two-dimensional and three-dimensional models

A two-dimensional model, such as that illustrated in Figure 5, can be used for the analysis of stresses and displacements in the rock surrounding a tunnel, shaft or borehole, where the length of the opening is much larger than its cross-sectional dimensions. The stresses and displacements in a plane, normal to the axis of the opening, are not influenced by the ends of the opening, provided that these ends are far enough away.

On the other hand, an underground powerhouse or crusher chamber has a much more equi-dimensional shape and the effect of the end walls cannot be neglected. In this case, it is much more appropriate to carry out a three-dimensional analysis of the stresses and displacements in the surrounding rock mass. Unfortunately, this switch from two to three dimensions is not as simple as it sounds and there are relatively few good three-dimensional numerical models, which are suitable for routine stress analysis work in a typical engineering design office.

EXAMINE3D (www.rocscience.com) is a three-dimensional boundary element program that provides a starting point for an analysis of a problem in which the three-dimensional geometry of the openings is important. Such three-dimensional analyses provide clear indications of stress concentrations and of the influence of three-dimensional geometry. In many cases, it is possible to simplify the problem to two-dimensions by considering the stresses on critical sections identified in the three-dimensional model.

More sophisticated three-dimensional finite element models such as FLAC3D (www.itascacg.com) are available, but the definition of the input parameters and interpretation of the results of these models would stretch the capabilities of all but the most experienced modellers. It is probably best to leave this type of modelling in the hands of these specialists.

It is recommended that, where the problem being considered is obviously three-dimensional, a preliminary elastic analysis be carried out by means of one of the three-dimensional boundary element programs. The results can then be used to decide whether further three-dimensional analyses are required or whether appropriate two-dimensional sections can be modelled using a program such as PHASE2 (www.rocscience.com), a powerful but user-friendly finite element program that generally meets the needs of most underground excavation design projects.

Examples of two-dimensional stress analysis

A boundary element program called EXAMINE2D is available as a free download from www.rocscience.com. While this program is limited to elastic analyses it can provide a very useful introduction for those who are not familiar with the numerical stress analysis methods described above. The following examples demonstrate the use of this program to explore some common problems in tunnelling.

Tunnel shape

Most contractors like a simple horseshoe shape for tunnels since this gives a wide flat floor for the equipment used during construction. For relatively shallow tunnels in good quality rock this is an appropriate tunnel shape and there are many hundreds of kilometres of horseshoe shaped tunnels all over the world.

In poor quality rock masses or in tunnels at great depth, the simple horseshoe shape is not a good choice because of the high stress concentrations at the corners where the sidewalls meet the floor or invert. In some cases failures initiating at these corners can lead to severe floor heave and even to failure of the entire tunnel perimeter as shown in Figure 8.

Figure 8: Failure of the lining in a horseshoe shaped tunnel in a highly stressed poor quality rock mass. This failure initiated at the corners where the invert meets the sidewalls.

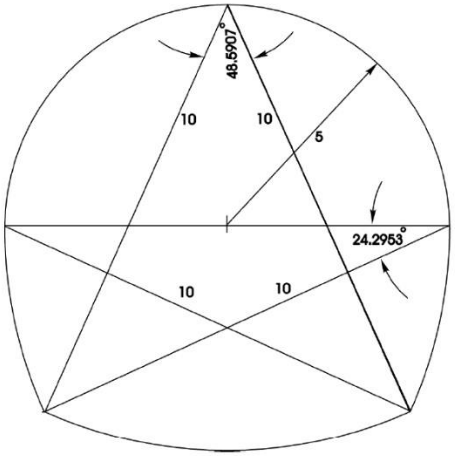

Figure 9: Dimensions of a 10 m span modified horseshoe tunnel shape designed to overcome some of the problems illustrated in Figure 8.

The stress distribution in the rock mass surrounding the tunnel can be improved by modifying the horseshoe shape as shown in Figure 9. In some cases this can eliminate or minimise the types of failure shown in Figure 8 while, in other cases, it may be necessary to use a circular tunnel profile.

Strength Factor vs Factor of Safety

$$S.F. = \frac{S_{max}}{S}$$

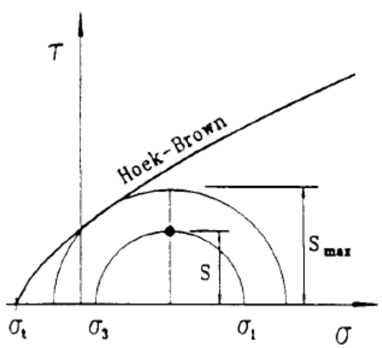

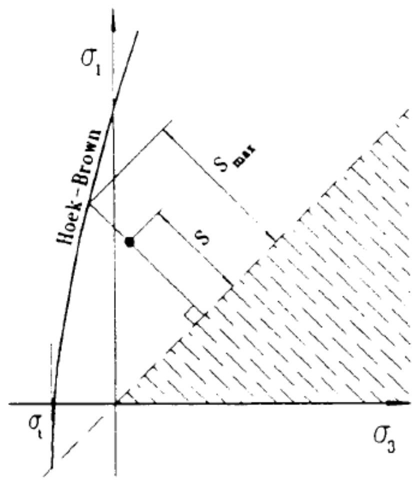

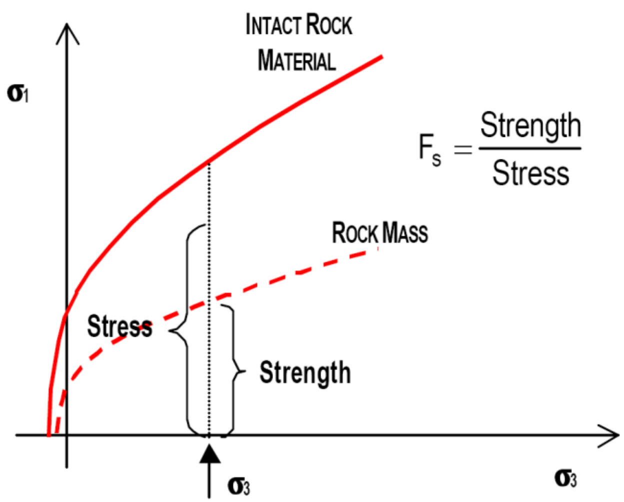

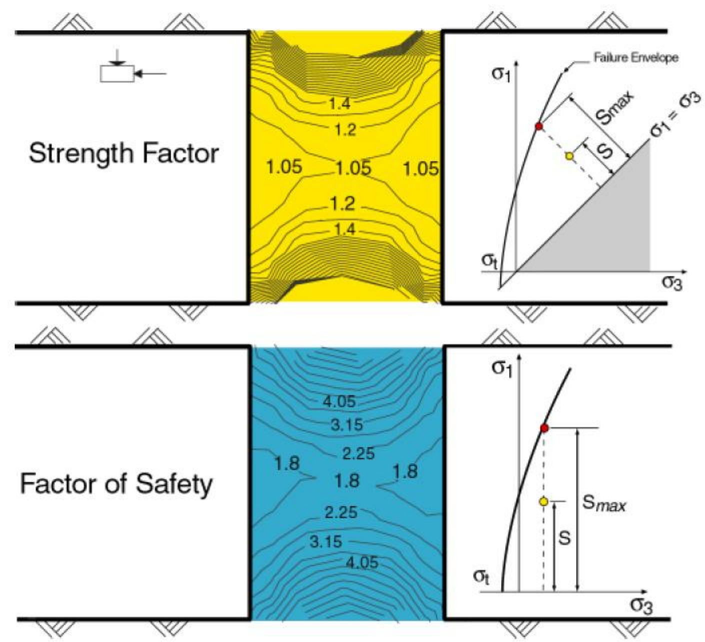

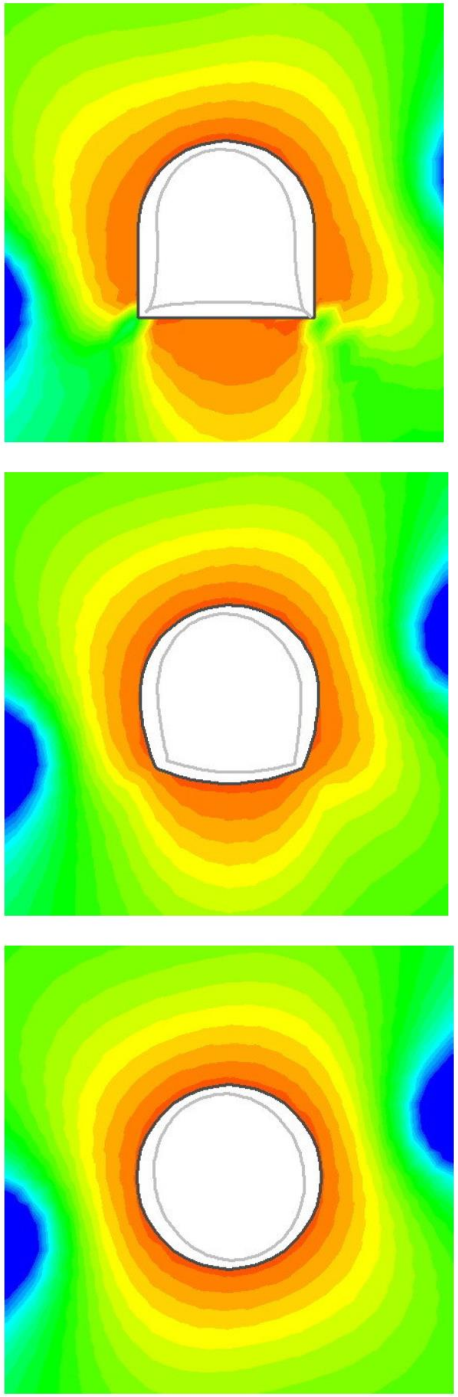

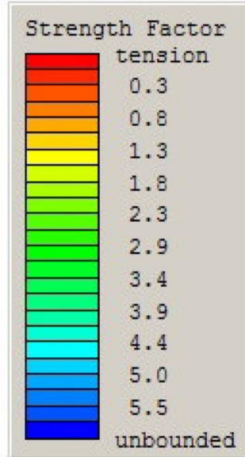

In situ stresses:

Major principal stress σ_1 = 10 MPa
Minor principal stress σ_3 = 7 MPa
Intermediate principal stress σ_2 = 9 MPa
Inclination of major principal stress to the horizontal axis = 15º

Rock mass properties:

Friction angle ϕ = 35º
Cohesion c = 1 MPa
Tensile strength = zero
Deformation modulus E = 4600 MPa

Figure 10: Comparison of three tunnel excavation profiles using EXAMINE2D. The contours are for the Strength Factor defined by the ratio of rock mass strength to the induced stress at each point. The deformed boundary profile (exaggerated) is shown inside each excavation.

The application of the program EXAMINE2D to compare three tunnel shapes is illustrated in Figure 10. Typical "average" in situ stresses and rock mass properties were used in this analysis and the three figures compare Strength Factor contours and deformed excavation profiles (exaggerated) for the three tunnel shapes.

It is clear that the flat floor of the horseshoe tunnel (top figure) allows upward displacement or heaving of the floor. The sharp corners at the junction between the floor and the tunnel sidewalls create high stress concentrations and also generate large bending moments in any lining installed in the tunnel. Failure of the floor generally initiates at these corners as illustrated in Figure 8.

Floor heave is reduced significantly by the concave curvature of the floor of the modified horseshoe shape (middle figure). In marginal cases these modifications to the horseshoe shape may be sufficient to prevent or at least minimise the type of damage illustrated in Figure 8. However, in severe cases, a circular tunnel profile is invariably the best choice, as shown by the smooth Strength Factor contours and the deformed tunnel boundary shape in the bottom figure in Figure 10.

Large underground caverns

A typical underground complex in a hydroelectric project has a powerhouse with a span of 20 to 25 m and a height of 40 to 50 m. Four to six turbine-generator sets are housed in this cavern and a cutaway sketch through one of these sets is shown in Figure 11. Transformers are frequently housed in a chamber or gallery parallel to the powerhouse. Ideally these two caverns should be as close as possible in order to minimise the length of the bus-bars connecting the generators and transformers. This has to be balanced against the size and hence the stability of the pillar between the caverns. The relative location and distance between the caverns is explored in the series of EXAMINE2D models shown in Figure 12, using the same in situ stresses and rock mass properties as listed in Figure 10.

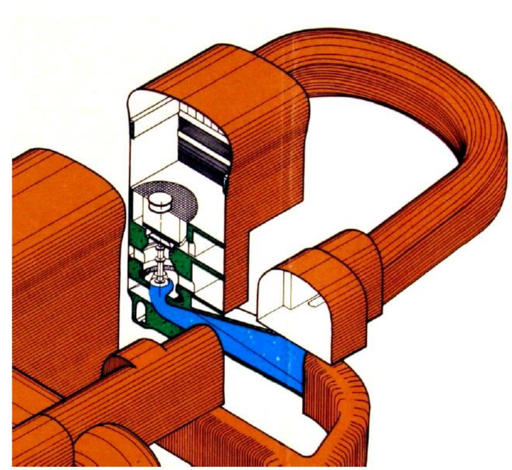

Figure 11: Cutaway sketch of the layout of an underground powerhouse cavern and a parallel transformer gallery.

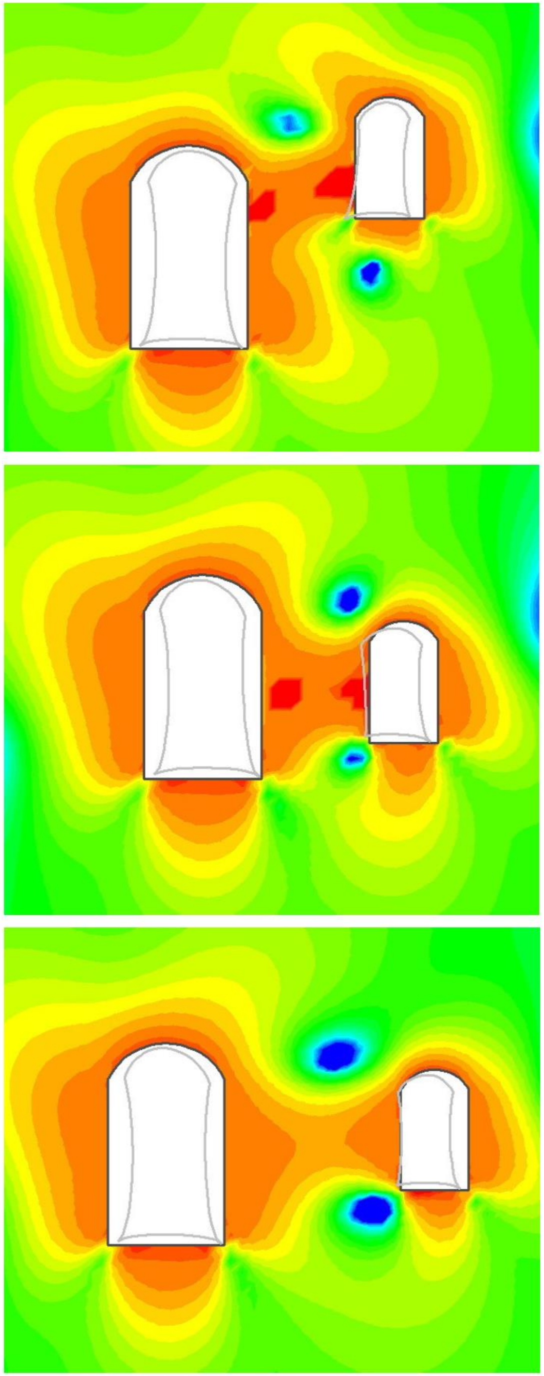

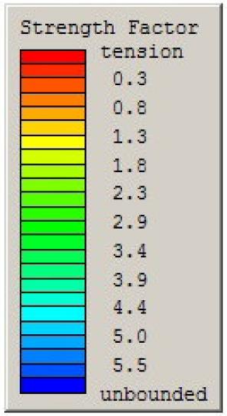

In situ stresses:

Major principal stress σ_1 = 10 MPa
Minor principal stress σ_3 = 7 MPa
Intermediate stress σ_2 = 9 MPa
Inclination of major principal stress to the horizontal axis = 15º

Rock mass properties:

Friction angle ϕ = 35º
Cohesion c = 1 MPa
Tensile strength = zero
Deformation modulus E = 4600 MPa

Figure 12: Comparison of three underground powerhouse and transformer gallery layouts, using EXAMINE2D. The contours are for the Strength Factor defined by the ratio of rock mass strength to the induced stress at each point. The deformed boundary profile (exaggerated) is shown inside each excavation.

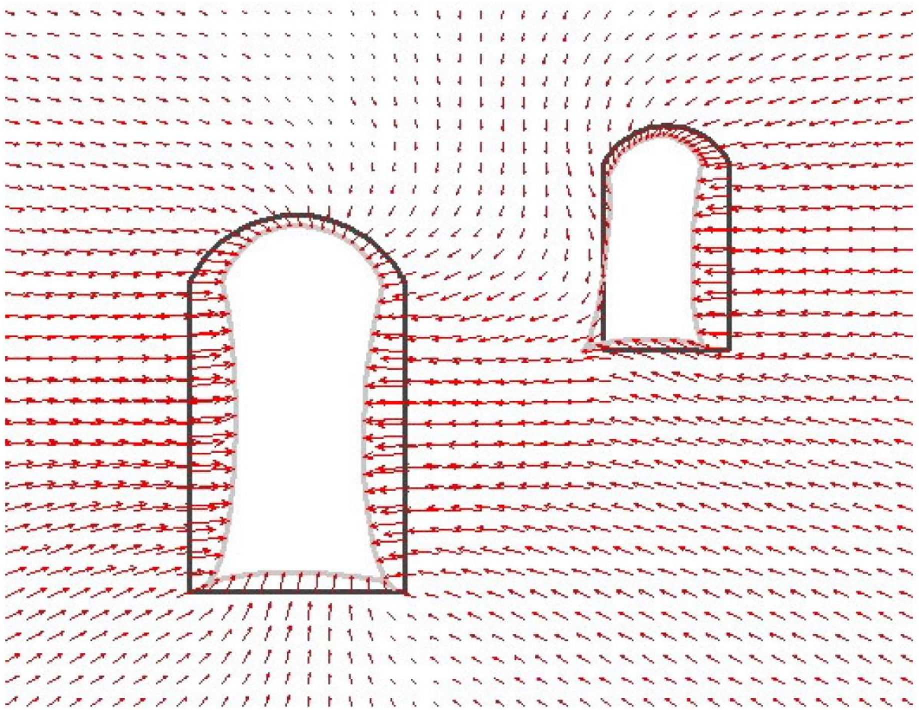

Figure 13: Displacement vectors and deformed excavation shapes for the underground powerhouse and transformer gallery.

A closer examination of the deformations induced in the rock mass by the excavation of the underground powerhouse and transformer gallery, in Figure 13, shows that the smaller of the two excavations is drawn towards the larger cavern and its profile is distorted in this process. This distortion can be reduced by relocating the transformer gallery and by increasing the spacing between the galleries as has been done in Figure 12.

Where the combination of rock mass strength and in situ stresses is likely to cause overstressing around the caverns and in the pillar, a good rule of thumb is that the distance between the two caverns should be approximately equal to the height of the larger cavern.

The interested reader is encouraged to download the program EXAMINE2D (free from www.rocscience.com) and to use it to explore the problem, such as those illustrated in Figures 10 and 12, for themselves.

Stress-Controlled Instability Mechanisms

Structurally-controlled instabilities are generally driven by a unidirectional body force, i.e. gravity. Stress-controlled instabilities, however, are not activated by a single force, but by a tensor with six independent components. Hence, the manifestations of stress-controlled instability are more variable and complex than those of structurally-controlled failures.

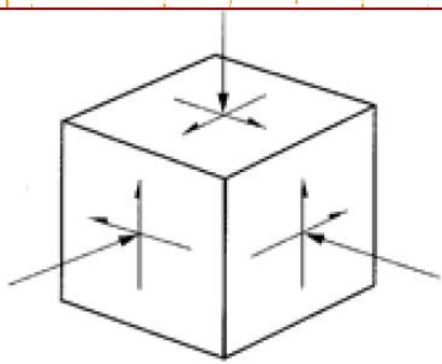

$$\begin{bmatrix} \sigma_{xx} & \tau_{xy} & \tau_{xz} \\ \tau_{yx} & \sigma_{yy} & \tau_{yz} \\ \tau_{zx} & \tau_{zy} & \sigma_{zz} \end{bmatrix}$$

Stress-Controlled Instability Mechanisms

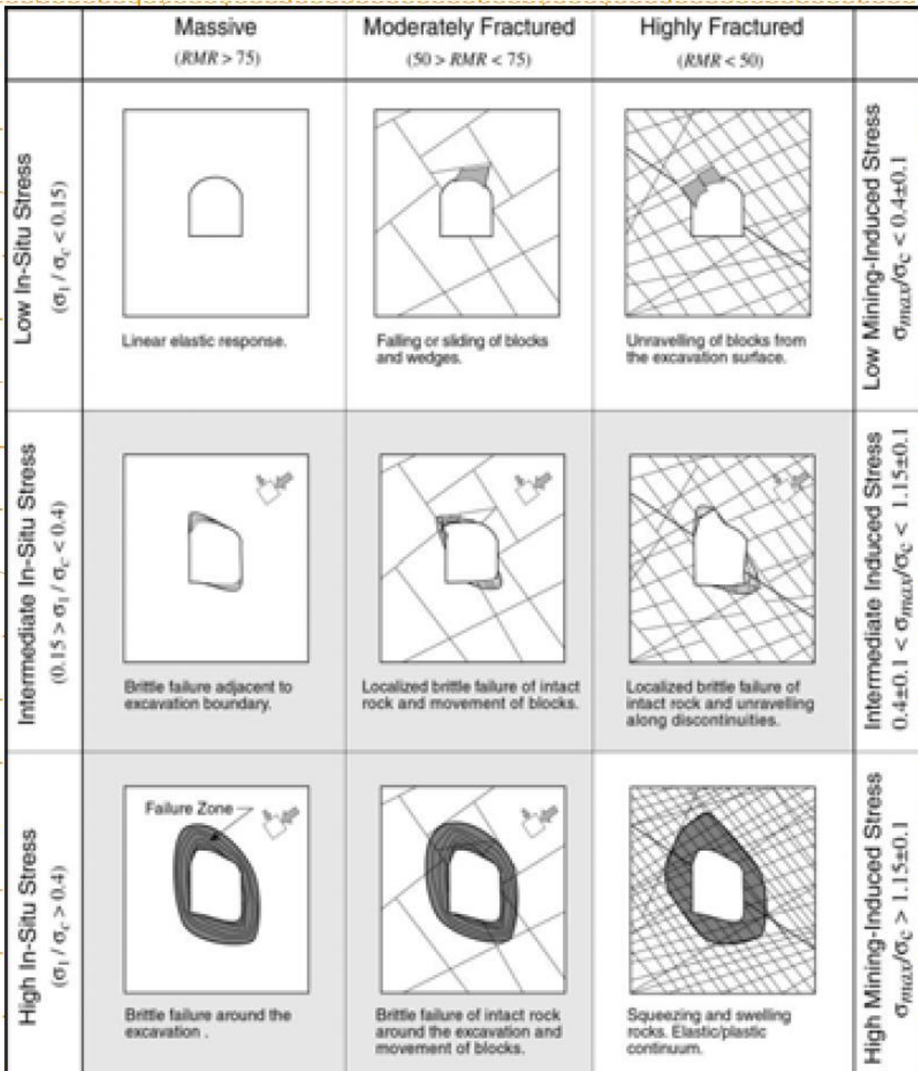

Kaiser *et al.* (2000)

Stress-Controlled Instability Mechanisms

Although the fundamental complexity of the nature of stress has to be fully considered in the design of an underground excavation, the problem can be initially simplified through the assumptions of continuous, homogeneous, isotropic, linear elastic behaviour (CHILE).

CHILE: Continuous, Homogeneous, Isotropic, Linear Elastic

DIANE: Discontinuous, Inhomogeneous, Anisotropic, Non-Elastic

The engineering question is whether a solution based on the CHILE assumption are of any assistance in design. In fact though, many CHILE-based solutions have been used successfully, especially in those excavations at depth where high stresses have closed the fractures and the rock mass is relatively homogeneous and isotropic. However, in near-surface excavations, where the rock stresses are lower, the fractures more frequent, and the rock mass more disturbed and weathered, there is more concern about the validity of the CHILE model.

Stress-Controlled Instability Mechanisms

A stress analysis begins with a knowledge of the magnitudes and directions of the *in situ* stresses in the region of the excavation. This allows for the calculation of the excavation disturbed or induced stresses.

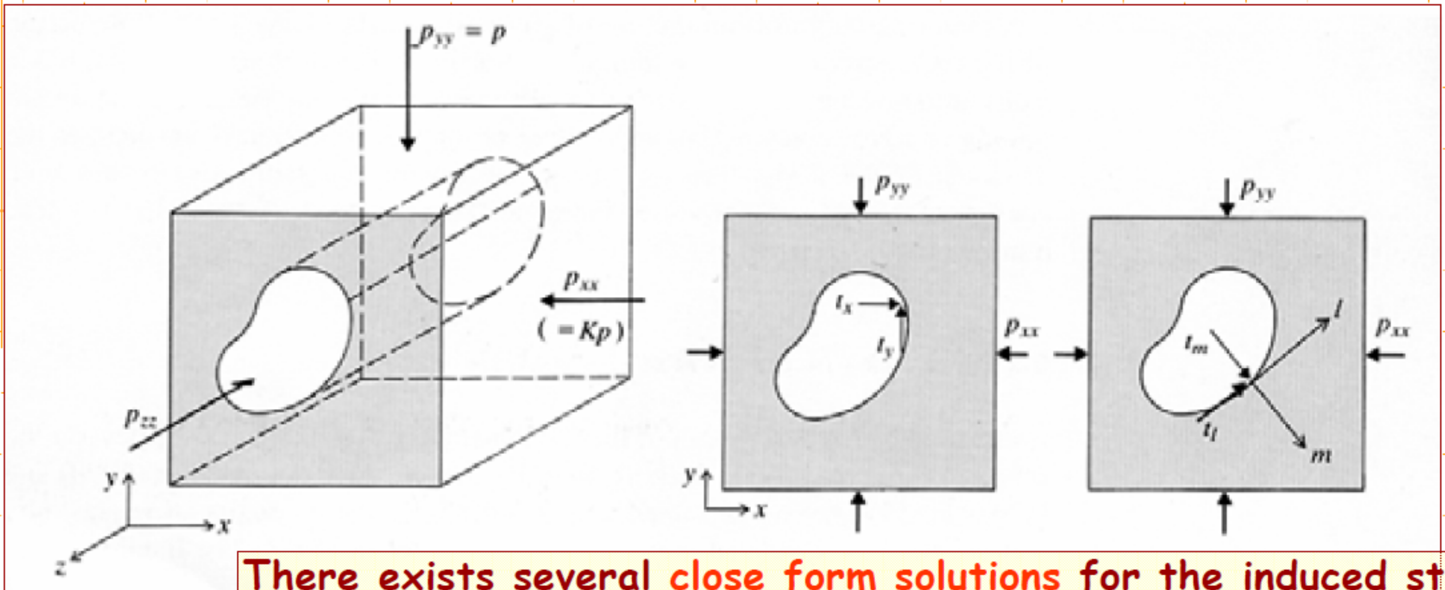

Brady & Brown (1993)

There exists several close form solutions for the induced stresses around circular and elliptical openings (and complex variable techniques extend these to many smooth, symmetrical geometries), and with numerical analysis techniques the values of the induced stresses can be determined accurately for any three-dimensional excavation geometry.

Stresses & Displacements - Circular Excavations

In rock mechanics, the Kirsch equations are the most widely used suite of equations from the theory of elasticity. They allow the determination of stresses and displacements around a circular excavation.

Stress ratio:
$k = \sigma_1/\sigma_3$

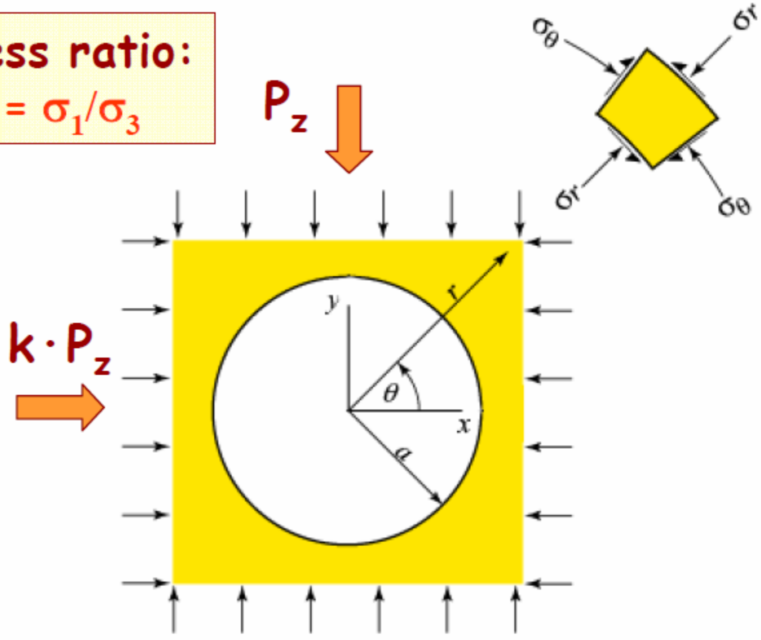

$$\sigma_r = \tfrac{1}{2}p_z \left\{(1+k)\left(1-\frac{a^2}{r^2}\right) - (1-k)\left(1-4\frac{a^2}{r^2}+3\frac{a^4}{r^4}\right)\cos 2\theta\right\}$$

$$\sigma_\theta = \tfrac{1}{2}p_z \left\{(1+k)\left(1+\frac{a^2}{r^2}\right) + (1-k)\left(1+3\frac{a^4}{r^4}\right)\cos 2\theta\right\}$$

$$\tau_{r\theta} = \tfrac{1}{2}p_z \left\{(1-k)\left(1+2\frac{a^2}{r^2}-3\frac{a^4}{r^4}\right)\sin 2\theta\right\}$$

$$u_r = -\frac{p_z a^2}{4Gr}\left\{(1+k) - (1-k)\left(4(1-\nu)-\frac{a^2}{r^2}\right)\cos 2\theta\right\}$$

$$u_\theta = -\frac{p_z a^2}{4Gr}\left\{(1-k)\left(2(1-2\nu)+\frac{a^2}{r^2}\right)\sin 2\theta\right\}$$

Stresses & Displacements - Circular Excavations

From these equations we can see that the stresses on the boundary (i.e. when $r = a$) are given by:

$$\sigma_r = 0$$
$$\sigma_\theta = p_z[(1+k) + 2(1-k)\cos 2\theta]$$
and $$\tau_{r\theta} = 0$$

Note that the radial stresses are zero because there is no internal pressure, and the shear stresses must be zero at a traction-free boundary.

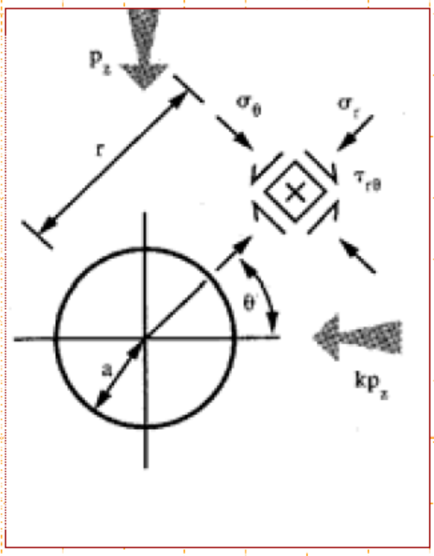

Max. Tangential Stress

$$\sigma_{\theta max}=3\sigma_1-\sigma_3 = 3(k-1)\sigma_3$$

Min. Tangential Stress

$$\sigma_{\theta min}=3\sigma_3-\sigma_1= 3(1-k)\sigma_3$$

Example #1: Stresses around a Circular Opening

Q. At a depth of 750 m, a 10-m diameter circular tunnel is driven in rock having a unit weight of 26 kN/m^3 and uniaxial compressive and tensile strengths of 80.0 MPa and 3.0 MPa, respectively. Will the strength of the rock on the tunnel boundary be exceeded if:

(a) k=0.3, and
(b) k=2.0?

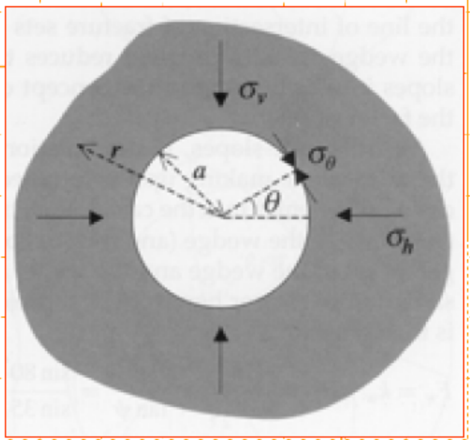

A. Since the tunnel has neither a support pressure nor an internal pressure applied to it, the local stresses at the boundary have $\sigma_3 = \sigma_r = 0$ and $\sigma_1 = \sigma_\theta$. The Kirsch solution for the circumferential stress is:

$$\sigma_\theta = \tfrac{1}{2}\sigma_v \left[(1+k)\left(1+\frac{a^2}{r^2}\right) + (1-k)\left(1+3\frac{a^4}{r^4}\right)\cos 2\theta \right]$$

Example #1: Stresses around a Circular Opening

Q. Circular tunnel: 750 m deep, 10m diameter, γ_{rock} = 26 kN/m^3, σ_{UCS} = 80.0 MPa, σ_T = 3.0 MPa. Will the strength of the rock on the tunnel boundary be reached if: (a) k=0.3, and (b) k=2.0?

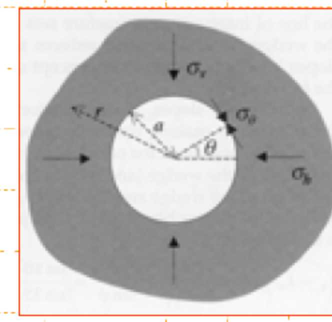

A.

$$\sigma_\theta = \tfrac{1}{2}\sigma_\nu \left[(1+k)\left(1+\frac{a^2}{r^2}\right) + (1-k)\left(1+3\frac{a^4}{r^4}\right)\cos 2\theta\right]$$

For a location on the tunnel boundary, where a = r, the Kirsch equation simplifies to:

$$\sigma_\theta = \sigma_\nu\left[(1+k) + 2(1-k)\cos 2\theta\right].$$

Example #1: Stresses around a Circular Opening

Q. Circular tunnel: 750 m deep, 10m diameter, γ_{rock} = 26 kN/m^3, σ_{UCS} = 80.0 MPa, σ_T = 3.0 MPa. Will the strength of the rock on the tunnel boundary be reached if: (a) k=0.3, and (b) k=2.0?

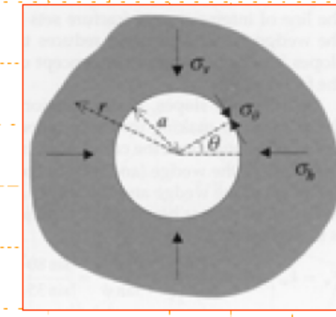

A. We assume that the vertical stress is caused by the weight of the overburden, in which case we have:

$$\sigma_v = \gamma\, z = 0.026 \times 750 = 19.5\ MPa$$

The extreme values of induced stress occur at positions aligned with the principal *in situ* stresses, and so in order to compute the stress induced in the crown and invert (i.e. roof and floor) we use θ = 90°, and for the sidewalls we use θ = 0° .

Example #1: Stresses around a Circular Opening

Q. Circular tunnel: 750 m deep, 10m diameter, γ_{rock} = 26 kN/m^3, σ_{UCS} = 80.0 MPa, σ_T = 3.0 MPa. Will the strength of the rock on the tunnel boundary be reached if: (a) k=0.3, and (b) k=2.0?

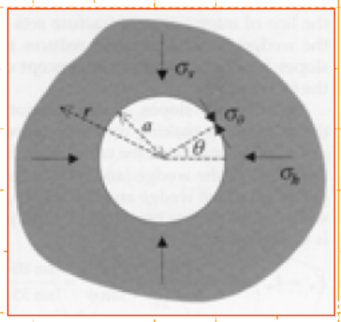

A. For k=0.3:

Crown and invert (θ = 90°), σ_θ = -1.95 MPa (i.e. tensile)
Sidewalls (θ = 0°), σ_θ = 52.7 MPa

For k=2.0:

Crown and invert (θ = 90°), σ_θ = 97.5 MPa

compressive strength is exceeded

Sidewalls (θ = 0°), σ_θ = 19.5 MPa

Stress and Failure Criterion

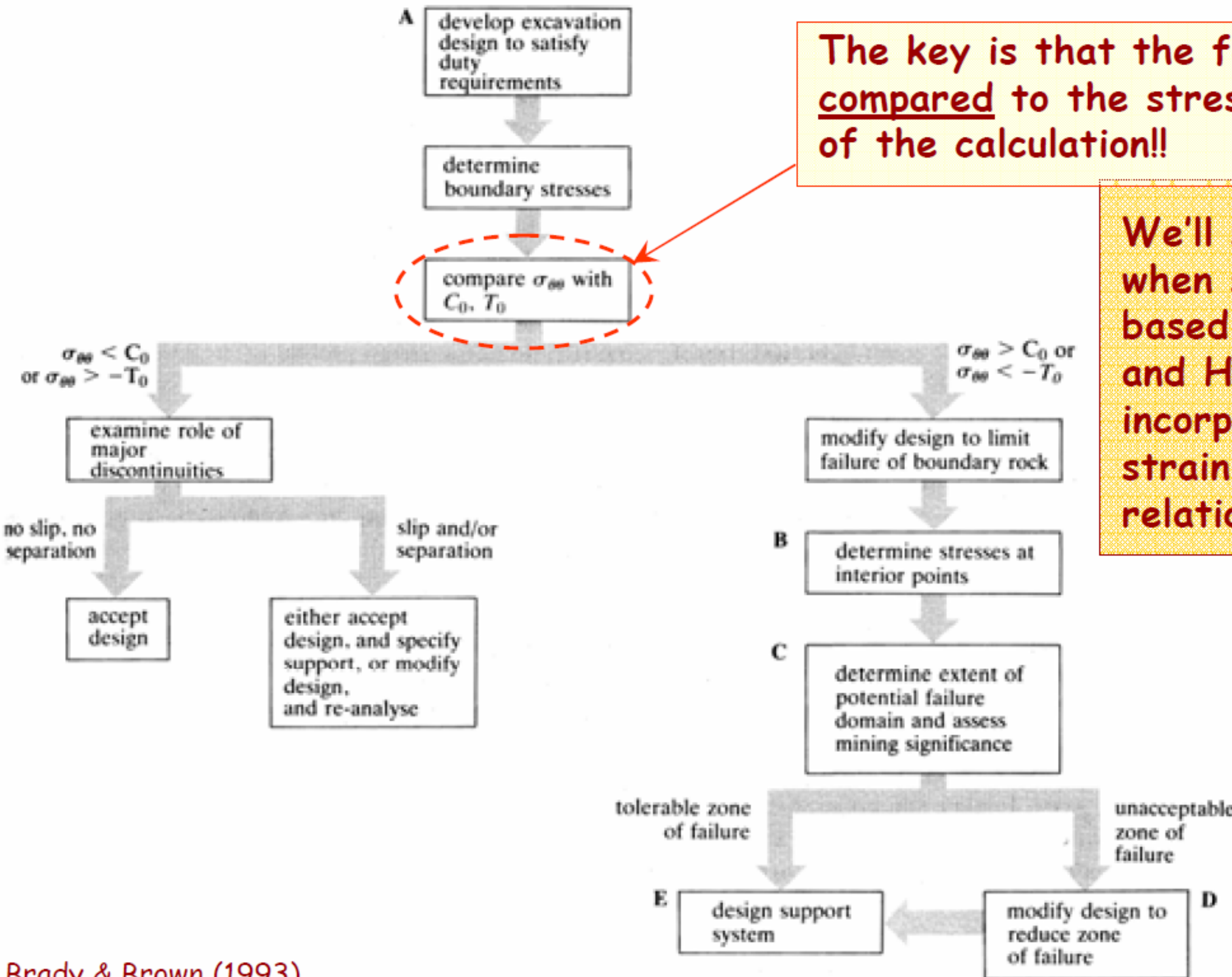

Brady & Brown (1993)

The key is that the failure criterion is <u>compared</u> to the stresses and is not part of the calculation!!

We'll see this is different when similar relationships based on Mohr-Coulomb and Hoek-Brown are incorporated into stress-strain constitutive relationships.

Stresses Away from Opening

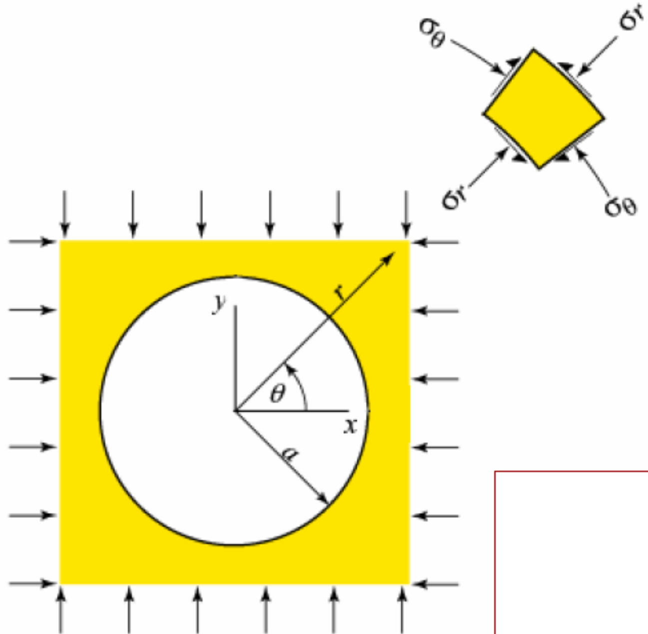

$$\sigma_r = \tfrac{1}{2} p_z \left\{ (1+k)\left(1 - \frac{a^2}{r^2}\right) - (1-k)\left(1 - 4\frac{a^2}{r^2} + 3\frac{a^4}{r^4}\right)\cos 2\theta \right\}$$

$$\sigma_\theta = \tfrac{1}{2} p_z \left\{ (1+k)\left(1 + \frac{a^2}{r^2}\right) + (1-k)\left(1 + 3\frac{a^4}{r^4}\right)\cos 2\theta \right\}$$

$$\tau_{r\theta} = \tfrac{1}{2} p_z \left\{ (1-k)\left(1 + 2\frac{a^2}{r^2} - 3\frac{a^4}{r^4}\right)\sin 2\theta \right\}$$

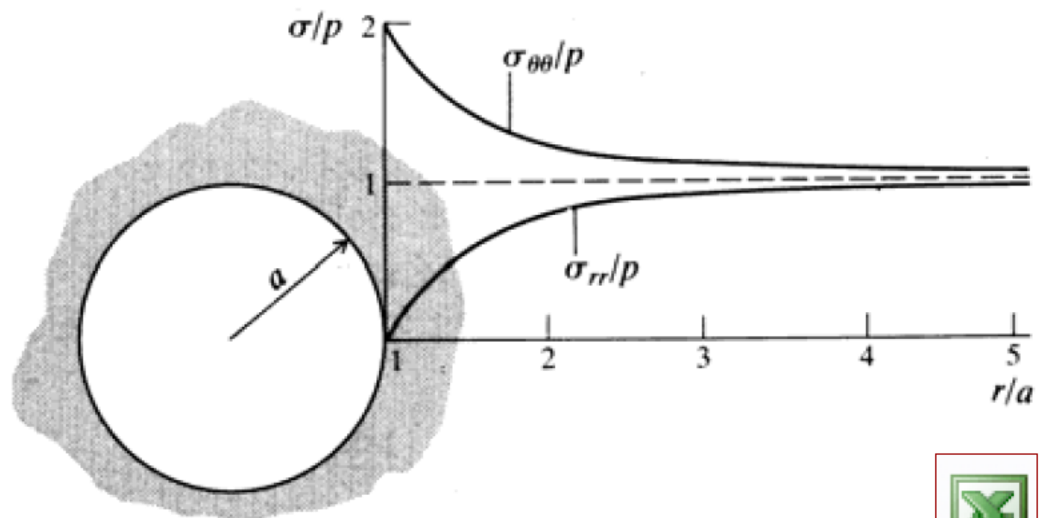

Zone of Influence

The concept of influence is important in excavation design, since the presence of a neighbouring opening may provide a significant disturbance to the near-field stresses to the point of causing failure.

... (a) axisymmetric stress distribution around a circular opening in a hydrostatic stress field; (b) circular openings in a hydrostatic stress field, effectively isolated by virtue of their exclusion from each other's zone of influence.

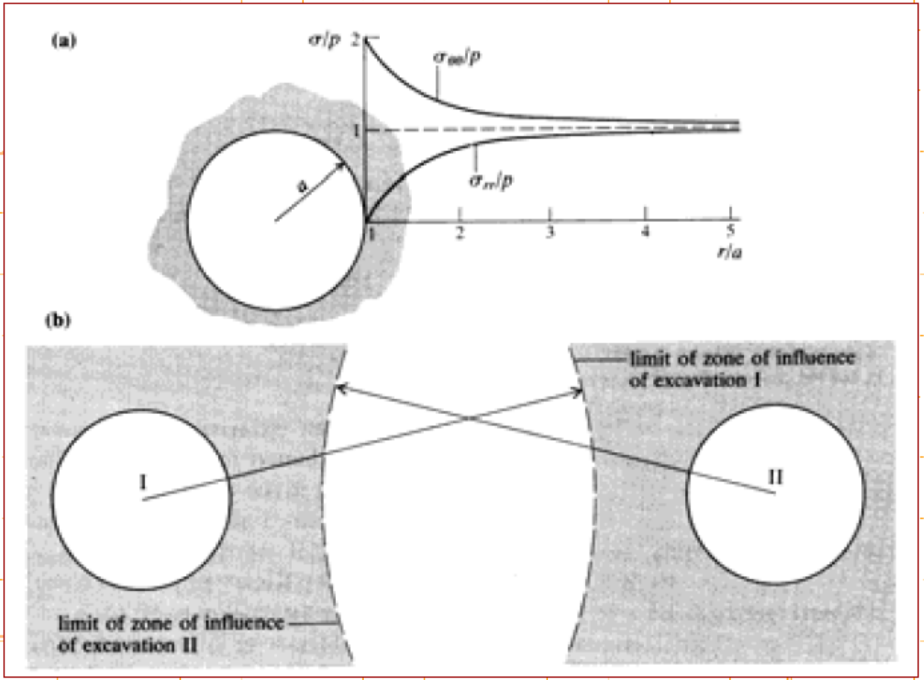

Brady & Brown (1993)

Zone of Influence

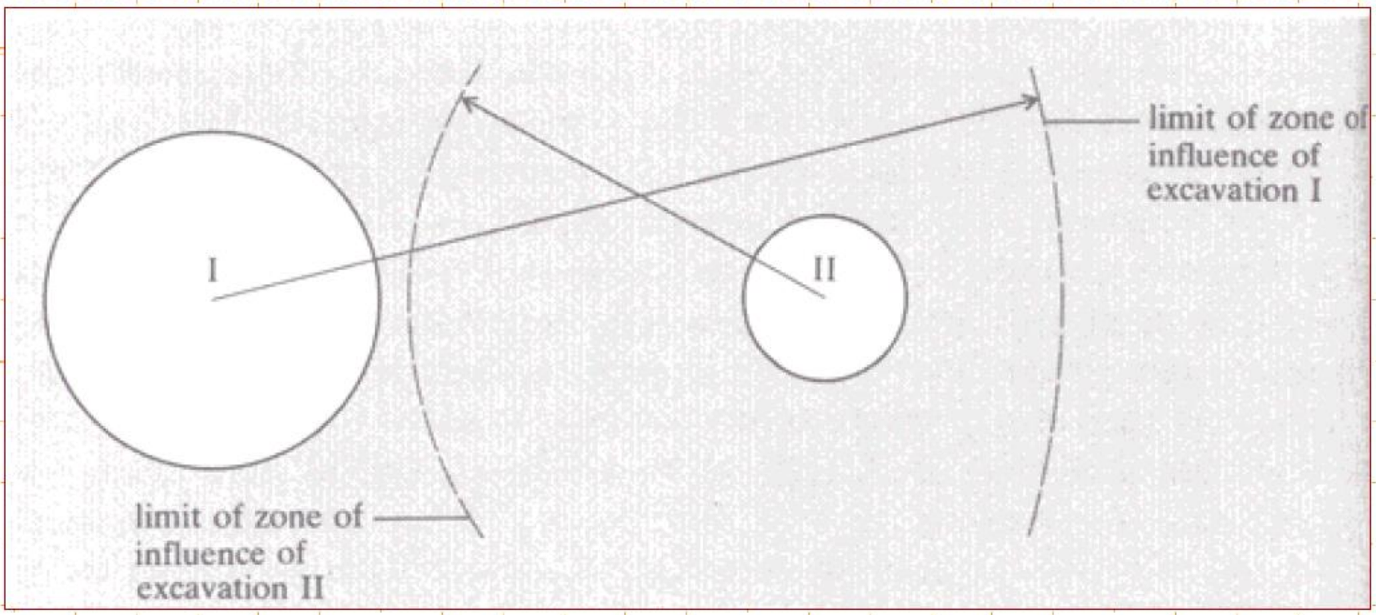

Brady & Brown (1993)

... illustration of the effect of contiguous openings of different dimensions. The zone of influence of excavation I includes excavation II, but the converse does not apply.

Stresses Around Elliptical Openings

The stresses around elliptical openings can be treated in an analogous way to that just presented for circular openings. There is much greater utility associated with the solution for elliptical openings than circular openings, because these can provide a first approximation to a wide range of engineering geometries, especially openings with high width/height ratios (e.g. mine stopes, power house caverns, etc.).

From a design point of view, the effects of changing either the orientation within the stress field or the aspect ratio of such elliptical openings can be studied to optimize stability.

Stresses Around Elliptical Openings

Assuming isotropic rock conditions, an elliptical opening is completely characterized by two parameters: aspect ratio (major to minor axis) which is the eccentricity of the ellipse; and orientation with respect to the principle stresses. The position on the boundary, with reference to the x-axis, is given by the angle χ.

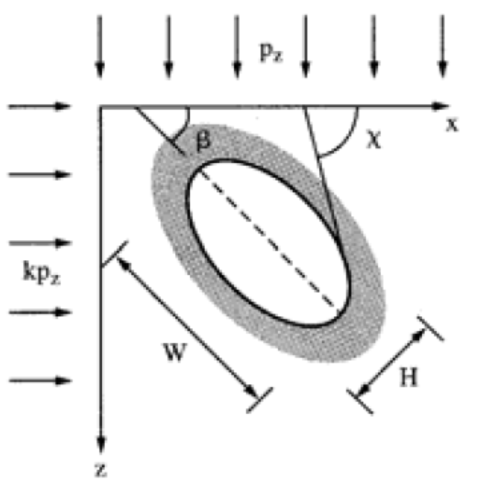

$$\sigma_\theta = \frac{p}{2q}\Big\{(1+k)\big[(1+q^2)+(1-q^2)\cos 2(\chi-\beta)\big] -(1-k)\big[(1+q)^2\cos 2\chi + (1-q^2)\cos 2\beta\big]\Big\}$$

where $q = \dfrac{W}{H}$

Hudson & Harrison (1993)

Stresses Around Elliptical Openings

It is instructive to consider the maximum and minimum values of the stress concentrations around the ellipse for the geometry of an ellipse aligned with the principal stresses. It can be easily established that the extremes of stress concentration occur at the ends of the major and minor axes.

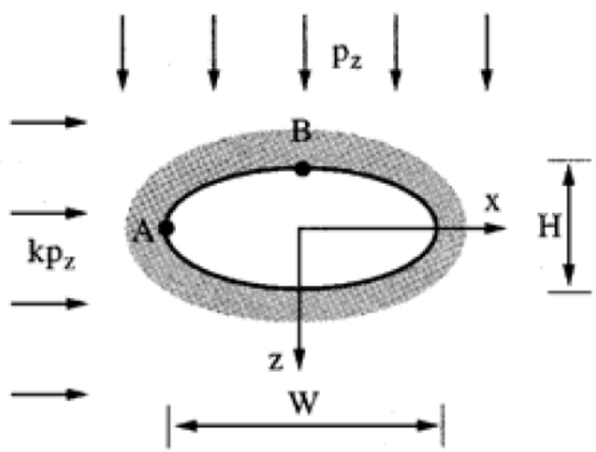

$$\sigma_A = p(1 - k + 2q) = p\left(1 - k + \sqrt{\frac{2W}{\rho_A}}\right),$$

$$\sigma_B = p\left(k - 1 + \frac{2k}{q}\right) = p\left(k - 1 + k\sqrt{\frac{2H}{\rho_B}}\right)$$

where, for an ellipse, the radii of curvature are

$$\rho_A = \frac{H^2}{2W} \text{ and } \rho_B = \frac{W^2}{2H}$$

Hudson & Harrison (1993)

Zone of Influence

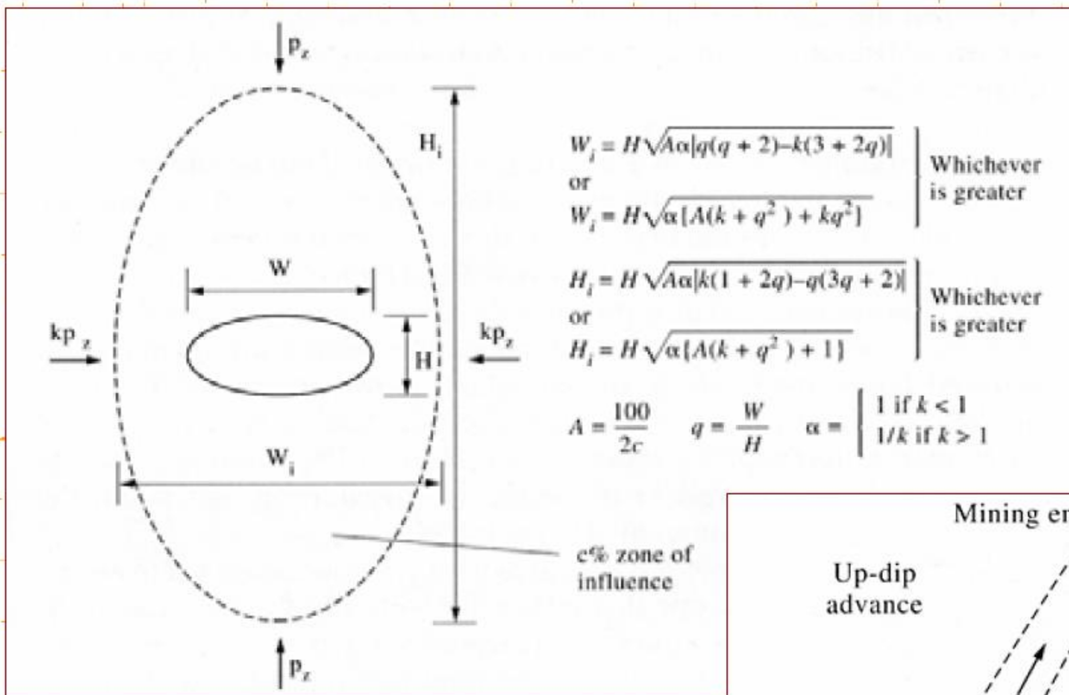

... elliptical approximation to the zone of influence around an elliptical excavation.

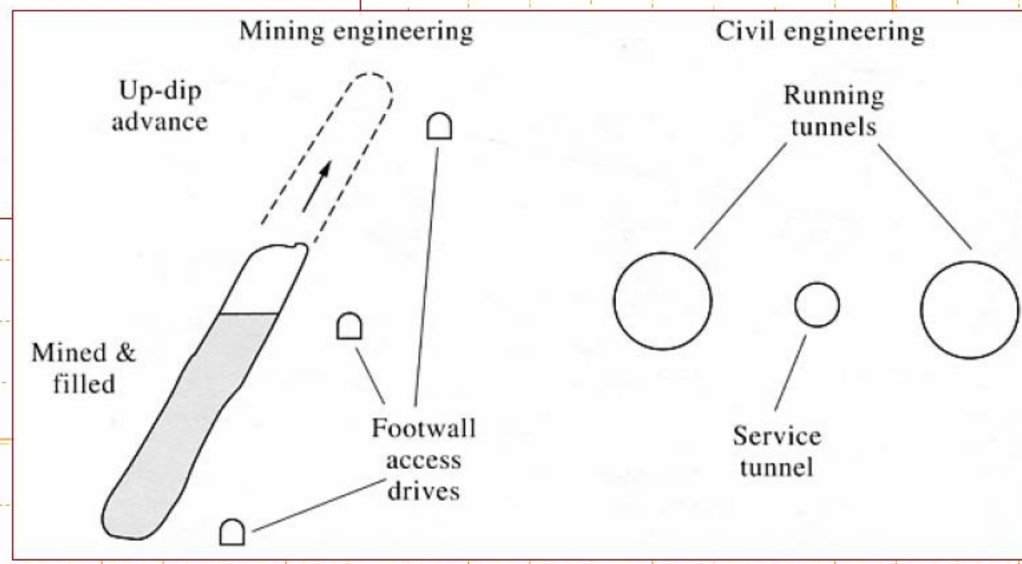

Hudson & Harrison (1993)

Numerical Modelling

Numerical methods of stress and deformation analysis fall into two categories:

Integral Methods

- incl. boundary-element method
- only problem boundary is defined & discretized
- Pro: more computationally efficient
  Con: restricted to elastic analyses

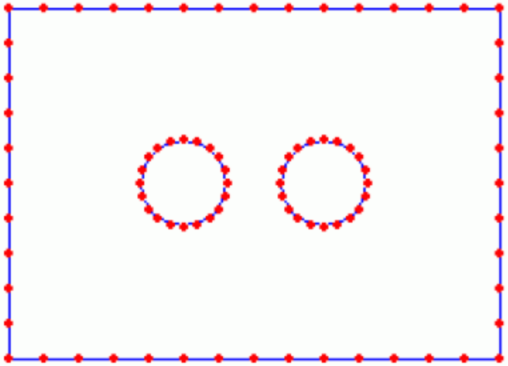

Differential Methods

- incl. finite-element/-difference & distinct-element methods
- problem domain is defined & discretized
- Pro: non-linear & heterogeneous material properties accommodated
  Con: longer solution run times

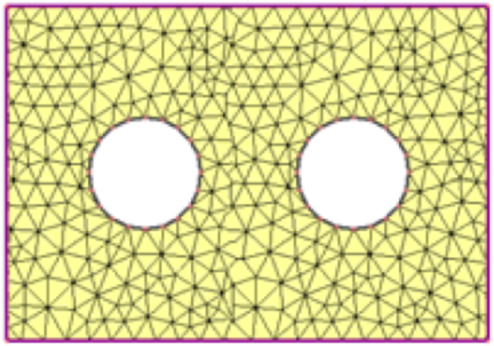

Stress Analysis & Failure